DESIGNING PULSE COUPLED OSCILLATORS TO SYNCHRONIZE

A Dissertation

Presented to the Faculty of the Graduate School

of Cornell University

in Partial Fulfillment of the Requirements for the Degree of

Doctor of Philosophy

by

Joel Daniel Nishimura

August 2013

DESIGNING PULSE COUPLED OSCILLATORS TO SYNCHRONIZE

Joel Daniel Nishimura, Ph.D.

Cornell University 2013

Oscillators exhibit some of the simplest dynamic behavior, yet systems of interacting oscillators are capable of intricate and complex behaviors. It is partly this elegance that has made them a frequent object of study, but also their ubiquity. In particular, pulse coupled oscillators (PCOs), where oscillator interactions occur at discrete times are particularly applicable. Not only do PCOs have applications in biological systems—such as the heart's pacemaker, flashing fireflies, and biological neural networks—PCOs have recently been adapted to control clocks inside wireless sensor networks [33, 21]. However, since traditional PCO models were designed to study synchronization abstractly, it is not surprising that they are no longer able to synchronize when exposed to real world settings. This thesis investigates the classic dynamical systems question of the synchronization of pulse coupled oscillators when classic dynamical systems tools no longer apply. Instead, utilizing a variety of nonstandard techniques, we design a new PCO model and prove strong theoretical results, which have applications in biology and the engineering of wireless sensor networks.

BIOGRAPHICAL SKETCH

Joel Nishimura was born May 1984 to Lois Harbaugh and Weston Nishimura. While technically born in Redmond Washington, he grew up in nearby Bellevue which is where he learned to describe his hometown to non-Washingtonians as simply Seattle. Coming of age in Seattle provided many opportunities to explore the pristine wilderness of the Pacific Northwest, whether that be fishing, hiking or skiing. Thusly, Joel has fond childhood memories of fishing for ling cod, rock cod and the occasional salmon on the calm waters of the Puget Sound and hiking amongst the emerald tapestries of the Cascade foothills.

Despite Joel's early difficulties learning to read, by his senior year in high school Joel was president of *Math*♣, Earthbound (the environmental club), and Knowledge Bowl and went on to graduate Valedictorian from Bellevue High School in 2003. It's worth noting this happened despite Joel's ongoing and complete confusion with how to use commas, his horrendous Spanish and his avid predilection for digital entertainment.

Motivated partly by the incredible affordability of his state school and partly by some random process he believes is inherent in all university choices, Joel chose to attend the University of Washington. During his first year at the University of Washington Joel was awarded the University of Washington freshman medal in the false hope that later Joel could leverage the award to win some kind of fancy fellowship and make the university look good. Subsequently, Joel dropped out of the bioengineering program and somewhat haphazardly decided to major in Mathematics. While taking a course on scientific computing Joel met professor and future mentor Nathan Kutz, with whom he would later publish a paper on optical parametric oscillators and travel to Rome. Additionally, Joel spent a month studying gender, race and class in Bangalore, India and,

at the egging of a fellow traveler, got his left ear pierced for $1.

Immediately following undergrad, Joel attended Cornell University, seeking a Ph.D in Applied Mathematics with adviser Eric Friedman. During his fourth year, and following a summer long buffet at Google, Joel followed Eric to Berkeley, where he was hosted by the EECS department at Berkeley. While at Berkeley Joel enjoyed the local food scene, highway 1 north of San Francisco and the easy travel to Seattle via the Oakland airport.

Nonetheless, Joel's primary grad school experience was Cornellian—taking classic Cornell courses such as Wines, Cooking, Badminton and Introduction to Riflery. During the lesson on how to cut potatoes into tournes Joel met his fiancée: Stephanie Chan.

Provided all goes well, Joel will start as Assistant Professor of Mathematics at Arizona State University in the Fall.

In memory of my grandmothers, Martie Weston and Mary Sue Harbaugh

ACKNOWLEDGEMENTS

This work would not exist without my Ph.D adviser, Eric Friedman, my thesis committee: Steve Strogatz, Kevin Tang and Jon Kleinberg and the National Science Foundation. Additionally, I would not have had the opportunity to attend Cornell without the help of my undergrad advisor Nathan Kutz.

I also acknowledge Enrique Mallada, Tim Novikoff and Johan Ugander for useful conversations and collaborations and EECS at UC Berkeley for their hospitality. This research has been supported in part by the NSF under grant CDI-0835706 and partly through the NSF IGERT fellowship program, administered at Cornell by professor John Guckenheimer.

I would like to thank the students of CAM for their positive attitudes and intellectual curiosity. In particular, fellow students Amy Cochran, Sarah Iams, Johan Ugander, Diarmuid Cahalane, Adam Chacon, Katie Sullivan, Danielle Toupo, Isabel Mette Kloumann, Gwen Spencer, and Matthew Holden were immensely helpful in ways beyond recounting.

Finally, this work wouldn't be possible without the support of my parents, Lois Harbaugh and Weston Nishimura, my sister April Nishimura my fiancée Stephanie Chan and her family Stacy and Sue Chan.

TABLE OF CONTENTS

LIST OF FIGURES

LIST OF SYMBOLS

Oscillator Variables and Functions:

i	oscillator index
$\phi_i(t)$	oscillator phase variable
$\phi^+(t)$	maximum oscillator phase variable
$\phi^-(t)$	minimum oscillator phase variable
$\rho(t)$	range of oscillator phases
$\Phi(t)$	vector of oscillator phases
$f(\phi)$	phase response curve
$x_i(t)$	oscillator phase and firing history
$\lambda_i^l(t)$	time of the lth firing of oscillator i
ω_i	oscillator speed variable
Ω	vector of oscillator speeds

Network Variables:

G	graph
V	vertices
E	edges
$P(u)$	predecessor of vertex u
$S(u)$	successors of vertex u
$N(u)$	neighbors (undirected) of u
r	the radius of a Random Geometric Graph

Key System Parameters:

t	time
τ	system time delay across a single edge
$H(\Phi)$	$1 + \tau$ time map
B_0	measure of phase response curve inhibition
B_1	measure of phase response curve excitation
B	when $B_0 = B_1 = B$
ρ_0	critical range of oscillator convergence
s	critical oscillator firing time
$\delta_n(p)$	critical degree for probability p convergence
η	probability distribution for initial oscillator phases

CHAPTER 1

INTRODUCTION

Thirty one miles south of exit 66 on I-40 E in Tennessee lies the entrance to Elkmont Road in the Great Smoky Mountain National Park. Each year during a two week period between May and June, thousands of visitors make this trip, board the mandatory shuttle bus at 7:00 pm and cover their flashlights with red or blue cellophane so that they get to witness fireflies enact an ancient light show [1]. Unlike every other firefly in North America, the firefly these visitors get to see, *Photinus carolinus*, not only flashes individually but conditions permitting, together in unison. Locals refer to it simply as The Light Show [11].

Yet, *Photinus carolinus* is not the only firefly in the world to be able to synchronize. In fact an arguably more impressive display is available on the other side of the globe, in the tropical jungles of Southeast Asia. As argued in the August 1935 edition of Science "the synchronous flashing of fireflies in Siam [is] the outstanding zoological phenomenon in a country that abounds in zoological features of great interest" [47].

Synchronization is not limited to fireflies though—it's a general phenomenon, common in systems from neurons to systems in electrical engineering. Synchronization can range from being a pathological breakdown, as in epilepsy [12] to one of vital importance, such as in the proper functioning of the heart's sinoatrial node [19, 5], to a framework to understand decentralized coordination more generally [33, 50]. The prevalence of synchronous behavior should not come as a surprise, it is in many ways one of the simplest expressions of coordination in time. While there are doubtless many ways to understand co-

ordination, few methods would be able to match the precision of first describing synchrony mathematically and then describing the emergence of synchronization analytically. Indeed, as shown in work dating back to Art Winfree [55], and continued by many others, notably Kuramoto [28] and Mirollo and Strogatz [33], synchronization can be succinctly described mathematically and such descriptions can provide a very strong understanding of the phenomenon, settling decades long philosophical debates [48]. In such situations, mathematical modeling is revelatory because it demonstrates concretely that a few basic terms in an equation are sufficient to account for an observed real world phenomenon.

Yet, despite the ease with which synchrony in particular idealized systems can be described mathematically it can be surprisingly hard to understand the features in large systems which support or detract from synchronous behavior. Indeed, there is no overarching theory that states what conditions are necessary and sufficient to achieve synchrony in complicated real world situations. Thus, when Hong and Scaglione proposed a synchronization protocol for a real world system based off of idealized models for firefly synchronization [21] there were a number of design decisions which the existing theories did not address. Yet design can be another area where mathematical modeling can make significant contributions.

As such, the goal of this thesis is to develop the theory of synchronization by addressing a design question relevant for modern applications of pulse coupled oscillators in wireless sensor networks. Namely, under natural engineering assumptions, what system converges to synchrony the most reliably and what guarantees can be given for this system's performance? Along the way we will revisit the not infrequent themes: that optimization in engineering settings can

yield results with biological relevance, and that bringing tools and approaches from a wide array of disparate fields can yield surprisingly strong results. Ultimately we will investigate a classical dynamical systems question: the synchronization of pulse coupled oscillators, when classic dynamical systems tools no longer apply. Instead, utilizing a variety of nonstandard techniques, we design the system and prove strong theoretical results, which have applications in biology and the engineering of wireless sensor networks.

The organization of the thesis is as follows:

In this introductory chapter we will review the basic framework for this study of synchronization, that of Pulse Coupled Oscillators (PCOs). In particular it is shown that the model of pulse coupled oscillators we use is a generalization of many previous models for pulse coupled oscillators. Additionally, the application of pulse coupled oscillator models to the synchronization of Wireless Sensor Networks is also reviewed. Finally, some results for pulse coupled oscillators are reviewed, with several significant results highlighted.

In Chapter Two we present work previously alluded to, but as yet unpublished, that discusses optimizing a system of PCOs to achieve synchrony. First, we review the details of the Genetic Algorithm we used to optimize the PCO system, covering both the representation and the fitness function used in the algorithm. In the second section we present the results of the Genetic Algorithm and discuss their implications for several separate questions.

Chapter Three expands on work published in [37]. Inspired by the results of the Genetic Algorithm we demonstrate that for particularly simple systems

there is a clear way to understand the local convergence of the system to synchrony. Subsequently we demonstrated a way to expand this argument to vastly more general PCO systems.

Chapter Four also expands on published work, this time from [38]. Overall this chapter shows that a more complete probabilistic understanding of the likelihood of synchronization can be formed by combining the results in the second chapter with techniques common from network theory. This probabilistic understanding is made fuller by the inclusion of a discussion of graphs where non-synchronous solutions are possible.

Taken as a whole this body of work combines thinking and techniques from network theory, dynamical systems, algorithms and machine learning to prove surprisingly strong results about coordination, structure and the design of large systems.

1.1 Pulse Coupled Oscillators

Oscillators exhibit some of the simplest dynamic behavior, yet systems of interacting oscillators are capable of intricate and complex behaviors. It is partly this elegance that has made them a frequent object of study, but also their ubiquity. In particular, pulse coupled oscillators (PCOs), where oscillator interactions occur at discrete times are particularly applicable.

1.1.1 Motivation for Pulse Coupled Oscillators

There are many situations where pulse coupled oscillators are a natural modeling choice. As discussed in [33] and the references therein the list of application includes situations such as fireflies, neurons, cardiovascular cells in the heart, particularly those in the sinoatrial node, neurons in certain regimes, and as discussed later, wireless sensor networks.

1.1.2 A Model of Pulse Coupled Oscillators

There are many different models of pulse coupled oscillators. Similar to [51, 37, 38, 43, 17, 10] the following version of integrate and fire oscillator gains generality and simplicity, but loses the structure of other oscillator models. From a design perspective, the primary benefit of this model is that it focuses all design considerations into a single mathematical function from $[0, 1] \to [-1, 1]$.

We begin by introducing an important constraint. Consider a strongly connected directed graph, $G = (V, E)$ with vertex set V, edge set E, and let $n = |V|$. Let $S(i)$ and $P(i)$ define the successors and predecessors of a node i in G and when the graph is undirected we refer simply to neighbors $N(i)$.

On top of this graph we place a pulse coupled oscillator at each vertex i, and associate to it the phase variable $\phi_i \in [0, 1]$. If oscillator i were left in isolation it would evolve at constant rate $\frac{\mathrm{d}\phi_i}{\mathrm{d}t} = 1$. When $\phi_i = 1$ we say that that oscillator 'fires', sending out a 'signal' to its successors, $S(i)$, after which it has its phase reset to 0. Time $\tau < \frac{1}{2}$ after a signal is sent, that signal reaches its destination

and any receiving oscillator, j, adjusts its current phase according to a phase response curve $f_{ij}(\phi)$ such that:

$$\phi_j(t^+) \rightarrow \phi_j(t^-) + f_{ij}(\phi_j(t^-)).$$

When multiple signals arrive simultaneously they are processed sequentially in random order. In general when $f(x) < 0$ we refer to the phase response curve as 'inhibitory' for that value of x. Likewise, when $f(x) > 0$ the curve advances the oscillator towards firing and we refer to the phase response curve as 'excitatory' for that value of x.

In this model, the fundamental difference between oscillator systems are the phase response curves. As will be shown later, it is possible to translate many standard oscillator models into the above, often times moving complexity in the other model's integration step of the oscillator into the phase response function.

While this model can incorporate any strongly connected directed graph G, a particularly interesting class of graphs are Random Geometric Graphs (RGGs). A random geometric graph of n nodes can be constructed by assigning each node a position in a d-dimensional unit cube uniformly at random and then connecting any nodes within a radius r of each other and are studied in depth in [40]. In particular, 2-dimensional RGGs resemble the possible configuration of a wireless sensor network where each sensor network mote has a broadcasting range and the motes' positions are scattered randomly and thus receive special attention in this thesis.

Illustrative Example

Suppose, for example, that there are two oscillators i and j, with $\phi_i(0) = .5$ and $\phi_j(0) = .75$. Also suppose $\tau = .05$ and

$$f_i(\phi) = f_j(\phi) = \begin{cases} -\phi & : \phi \in [0, .5) \\ .5(1 - \phi) & : \phi \geq .5 \end{cases}$$

The system moves forward in a series of events:

time	ϕ_i	ϕ_j	
0	.5	.75	
.25	.75	$1 \rightarrow 0$	j fires
.3	$.8 \rightarrow .9$	.05	signal arrives at i
.4	$1 \rightarrow 0$	.15	i fires
.45	.05	$.2 \rightarrow 0$	signal arrives at j
1.05	.65	.6	

Notice that nothing interesting happens between the times when oscillators fire and signals arrive. In this way a delayed differential equation, which might otherwise appear infinite dimensional, is most often only finite dimensional, and easily implemented as an event driven simulation. Notice also, that after a single round of firing, the resulting oscillator phases are closer to each other.

Relationship to Other PCO Models

This model of pulse coupled oscillators is general enough to encapsulate many different pulse coupled oscillator models. For example, the integrate and fire

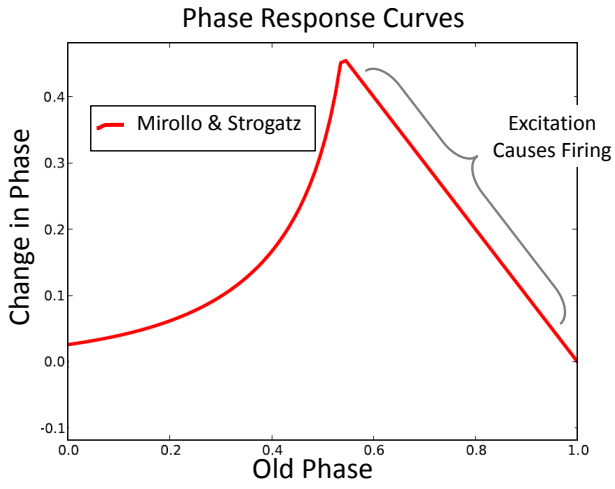

Figure 1.1: The PCO model we consider includes the popular integrate and fire models.

oscillator proposed by Peskin in [41] and extended in [33] can be formulated as oscillators with $\frac{d\phi_i}{dt} = 1$ and the phase response curve:

$$f(\phi) = -\phi + \min\{1, U^{-1}(U(\phi) + \epsilon))\}$$

where U is a charging curve that is monotonic increasing and concave down. In particular, Peskin used:

$$U(\phi) = C(1 - e^{-\gamma\phi})$$

for parameters C and γ. For a particular choice of ϵ, C and γ this leads to a phase response curve as seen in figure 1.1, notice that it is exclusively excitatory.

This charging curve model for pulse coupled oscillators is particularly important because it served as the conceptual foundation for wireless sensor network synchronization protocols in [21].

1.2 Wireless Sensor Networks

The promise of wireless sensor networks is to provide a cheap, efficient and unobtrusive way to gather information across space. Composed of many separate motes the purpose of a wireless sensor network as a whole can typically be understood from examining each individual mote. In principle each mote contains at least a wireless antenna, a power source (almost always a battery), and a sensor. Using the sensor, the mote records some phenomenon, communicates these observations with its neighboring motes and relies on the battery to power these activities. Since in many applications battery power is severely limited, there is typically a trade off between utilizing power reserves for communication and for sensing. To get a sense of the physical scale for a mote an example of a commercial network antenna used in wireless sensor networks is displayed in figure 1.2. Additionally, it's also possible to purchase already assembled sensor networks from specialized companies such as libelium. For example, one such wireless sensor network can be used to measure radiation levels [15]. Indeed, this example of a sensor network is particularly compelling because monitoring radiation levels can be important, and yet has traditionally required some degree of danger or extensive foresight and expensive installation.

The key difference between wireless sensor networks and other potential wireless sensor platforms is that communication in the network primarily occurs between nearby motes, and not directly with a centralized controller. Thus, coordination protocols must be decentralized and given the battery constraints, operate on as low an energy budget as possible. Despite these two complicating constraints, coordination is vital to the correct operation of most sensor nets. As

Figure 1.2: A wireless antenna, about the size of a quarter frequently used in wireless sensor networks. Image by Mark Fickett (Own work) [CC-BY-3.0 (http://creativecommons.org/licenses/by/3.0)], via Wikimedia Commons.

discussed before, one of the simplest questions of coordination is synchronization and it turns out synchronization is a useful goal for sensor nets.

1.2.1 The Utility of Synchronization in Sensor Networks

Synchronizing clocks on wireless sensor networks can provide several distinct benefits: increasing the accuracy of the data collected from the network; extending the battery life of motes in the network; and allowing for coordinated signal boosting.

For many potential sensing applications coordinating time is important because accurate time stamps are required to solve an inference problem. For ex-

ample, Nunez et al. demonstrate that if the goal of a sensor network equipped with microphones is to infer the location of a sudden and loud noise (such as a gunshot) then controlling clock errors is incredibly important [39]. Figure 1.3 displays the simulation results of Nunez et al. showing that errors in clock timing as small as $13\mu s$ can greatly impact accurate triangulation.

Similarly, accurate time stamps are important for determining direction of wavefronts and causality in general.

Synchronization can also be used to significantly increase the battery life in wireless sensor networks. In some wireless sensor networks, passive sensing for radio signals can consume significant portions of battery life. One potential strategy to save power is to intelligently time sensor net motes to enter and exit 'sleep' states during which the mote turns off its radio receiver [42]. While this can be a complicated control problem, there is a simple strategy for a synchronized system. The key being, that once synchronized, motes can simply confine all communication to lay within specified portions of their period, and synchronization grants that all other motes then know when to power up their receiving radios [52].

Another interesting possible application of synchronization in a wireless sensor network is 'cooperative reachback'. In cooperative reachback a group of motes is able to send a signal farther than any individual mote by timing their signals to constructively interfere [20]. Interestingly, it was this use of synchrony that first led Hong and Scaglione to draw inspiration from the natural world and suggest a new method of synchronizing clocks in wireless sensor network [20].

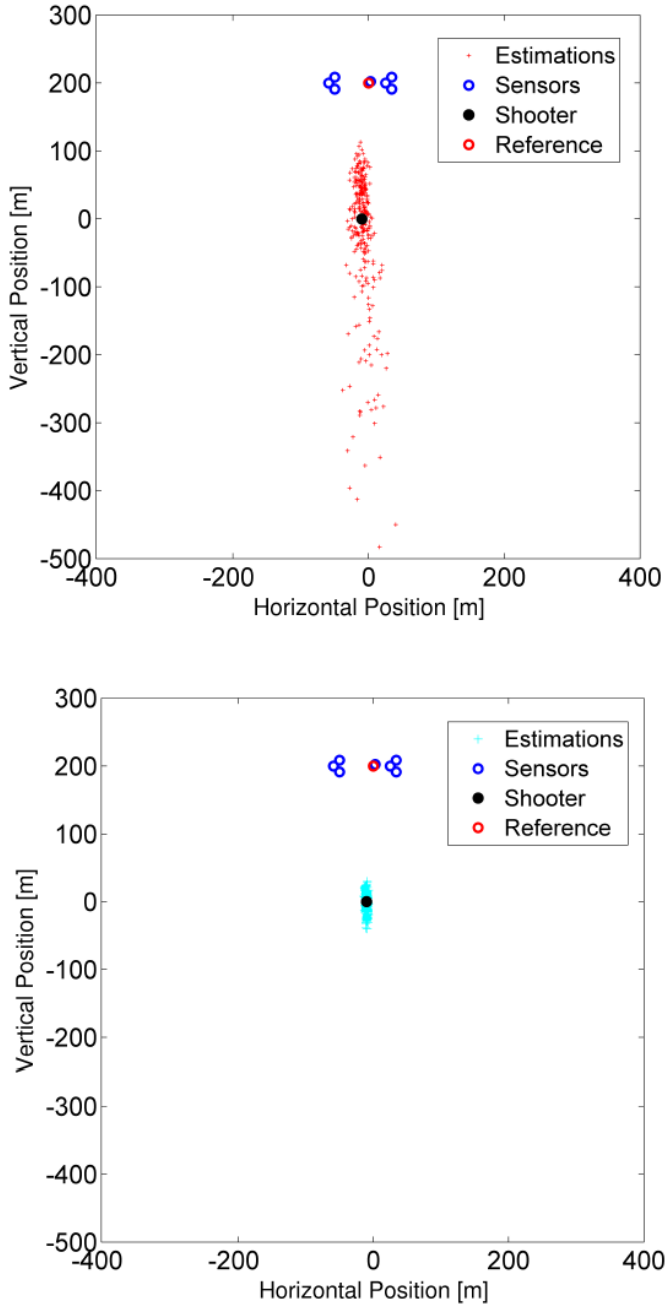

Figure 1.3: Estimates for a shooter location when the variance of the sensor net clocks is (a) $13\mu s$ and (b) $1.7\mu s$. Images from Nunez et al. [39] © 2012 IEEE.

1.2.2 Synchronization via Pulse Coupled Oscillators

Inspired by the guarantees of synchronization given by the results in [33] Hong and Scaglione proposed using a integrate and fire coupled oscillator located at each mote as the basis for a synchronization protocol, first in [20], and later in [21]. This approach has several distinct advantages:

- Inherently decentralized
- Resilient to individual mote failure
- Signals consist of individual bits
- Signal processing can be implemented in hardware

In order to adjust pulse coupled oscillators Hong and Scaglione added refractory periods, searched parameter space and performed numerous numerical trials. Following their work there has been significant efforts to further refine PCO protocols for synchronization and their eventual use in wireless sensor networks as discussed in the following section.

However, it turns out that the purely excitatory model of PCOs from [33] does not support exact synchrony as a solution in systems with both time delay and complex network topology. Thus, for a system with delay and complex topology we consider the more general model introduced above.

Conditions for Synchrony

Let the system be called 'synchronous' if for all time $t > t_0$, $\phi_i(t) = \phi_j(t)$ for all i, j. In order for synchrony to be a solution for general strongly connected graphs in the model we introduced above, it must either be the case that $f(\tau) = 0$, or $f(\tau + f(\tau)) = 0$, otherwise oscillators with a single incoming edge would receive different phase response than those with multiple incoming edges. Notice, synchrony is periodic with period $1 + f(\tau)$. Other approaches broaden the possible values of $f(\tau)$ by adding features to the oscillator model such as assuming that oscillators normalize incoming signals [50] or, as demonstrated later, by including a quiescent period.

1.3 Recent Pulse Coupled Oscillator Results

There is an extensive literature on pulse coupled oscillators, much of which focuses on models without time delay. Some theoretical treatments of pulse coupled oscillators with delay can be found in [29, 50, 56]. In regards to traditional dynamical systems techniques, of particular note is [50] which lays out detailed descriptions of local stability in integrate and fire oscillators on networks with delay. Central to the methods used in [50] are assumptions that oscillators are able to normalize their coupling strengths which is a reasonable assumption in neurons but more onerous for sensor nets. Additionally, the results in [50] demonstrate that understanding linear stability requires understanding a combinatorial explosion of different linear operators about synchrony. Meanwhile, the goal of engineering a system to converge to synchrony while using a mini-

mum number of signals, and having the simplest possible nodes leads naturally to investigating large coupling. For these reasons, typical dynamical systems techniques have recently been eschewed in favor of largely ad-hoc methods for analyzing new PCO systems designed for synchronization.

In particular, the synchronization of wireless sensor networks has motivated a number of new PCO system designs. It is common to augment the PCO system with things such as, several bits of memory [9, 22], infinite spatial density [22] or local knowledge of the network [50, 22]. While these studies have shown linear stability [50], or other forms of local convergence [9, 22], global convergence in these settings has either been shown to be impossible [50], requires stochastic and arbitrarily small delays [25] or remains unknown.

Alternatively, a class of oscillators with Type II phase response curves (PRCs), have been connected to synchronizing behavior theoretically [2, 16, 25] and in nature [49, 18, 46, 19, 3]. The distinguishing feature of oscillators with Type II PRCs is that an oscillator's phase can either be decreased (inhibited) or increased (excited), depending on the internal state of the oscillator. Indeed, the discovery that type II phase response curves are particularly well suited for handling complex topologies and time delay has led to a number of recent results, each at the forefront of pulse coupled oscillator convergence [37, 38, 25, 54, 53]. The results of [37, 38] are included in chapters 3 and 4 of this thesis.

Of these, it is important to consider the results of Klinglmayr and Bettsetter in [24], which discovered the importance of including stochastic signal error, later expanded in [25]. In particular Klinglmayr, Kirst, Bettstetter and Timme show in [25] that incorporating both stochastic signal error and phase response

curves that mix inhibition and excitation can lead to global convergence results for general graphs and a stochastic range of signal delays. Indeed, [25] is the first proof for global convergence in a difficult setting that includes both complex topology and delays. In order to guarantee convergence the authors utilize a phase response with excitation and inhibition to bring oscillator phases within a fixed error of each other. Once inside of this fixed error regular processing of signals only bring oscillators closer together when the stochastic delays approach 0. Meanwhile, the random signal error can be used to prevent the worst case non-synchronous solutions discussed briefly in chapters 3 and 4. However, it is unclear how onerous the requirement for stochastic signals, and arbitrarily small signal delays would be in worst case situations. For example, on a large enough star graph with particularly unfortunate initial conditions the probability that stochastic signal failures knocks the system towards synchrony can be exponentially small. Similarly arbitrarily small delays prevent many real world applications. It is likely that future research in this area will address these issues.

Another interesting research direction comes from continuously coupled oscillators. In [32], Mallada and Tang design a system of continuously coupled oscillators that adjust both phases and frequencies. By designing the frequency adjustments to implement a consensus algorithm the system is able to guarantee convergence in frequencies. Similarly the phase adjustments are designed according the criterion in [31] thereby guaranteeing that once frequencies converge, phases converge to synchrony. Furthermore, the authors demonstrate that a system clock synchronization scheme informed by their PCO system performs excellently at synchronizing server system clocks [30], even overcoming the well known problems associated with timing loops. While results from continuously coupled oscillators bear on pulse coupled oscillators in a weak

coupling limit, its currently unclear how to translate these results to a strongly coupled pulse coupled situations. Furthermore, it may be that implementing the frequency adjustment in a pulse coupled oscillator situation requires more communication than the single bit often assumed in PCO models and therefor may be better suited for the server applications where power considerations are less important. Nonetheless this recent work represents a promising possible direction for the study of PCO systems.

The work in this thesis builds on these recent trends, including as chapters the work in [37] and [38]. Additionally, the Genetic Algorithm numerical experimentation that motivated a renewed interest in type II phase response curves for sensor net applications is detailed in the following chapter.

CHAPTER 2

THE OPTIMIZATION OF PULSE COUPLED OSCILLATORS VIA A GENETIC ALGORITHM

Since there are features of the real world that complicate the synchronization described in [33, 21], if PCOs are to be used in wireless sensor networks it is important to consider new models of PCOs robust to these complicating features. In our framework searching for a more robust PCO model is tantamount to searching for different phase response curves. Given that the space of phase response curves is infinite dimensional it is not unreasonable to hope that there would be at least one such curve that could handle PCO convergence robustly. Yet, the sheer size of the infinite dimensional search space makes such a search daunting for manual inspection. For this reason in our search for phase response curves we employ a Genetic Algorithm (GA) modeled after one designed to infer natural laws of motion for experimental data [44].

In this chapter, it is shown that optimizing the shape of phase response curves offers, not only an answer to engineering questions, but sheds light on phase response curves generally. Based off these conclusions, we predict that those biological systems of pulse coupled oscillators, whose function is to synchronize, will belong to a class we call "strong type II" (STII). Indeed, our results demonstrate that strong STII PRCs are, in a very concrete sense, learnable.

In regards to learnability, we show that these curves are learnable in two different ways. First, we use a genetic algorithm to find the phase response curve that lead to synchrony on a random geometric graph. These algorithms resulted in strong STII and strong resetting curves. To verify that this wasn't

simply a peculiarity of the genetic algorithm, we also check the local energy landscape, demonstrating that there are clear gradients that can be followed.

Furthermore, we show that both delay and complex topology are extremely important features to include in order to avoid over-fitting the phase response curves. Optimization attempts without both complex topology and delay are prone to producing solutions that are fragile to increasing system complexity.

2.1 Methods

Genetic algorithms are a general purpose optimization routine which aims to emulate evolution by natural selection [34]. During the course of a genetic algorithm a set, or 'population' of potential solutions is maintained and at each time step, the poor performing solutions are replaced by recombinations of better performing solutions. The principle ingredients required for a genetic algorithm are a representation for solutions and an objective or fitness function. Together the representation and the fitness function define the particular problem that the GA is attempting to optimize. Additionally, the implementation of the GA is defined by specifying the schemes for crossover, mutation, selection and termination along with several other parameters.

2.1.1 Phase Response Curve Representation

In order to allow a computer to find a phase response curve that finds synchrony, it's necessary to represent phase response curves in a computer's mem-

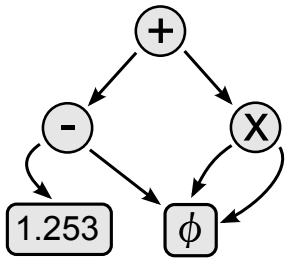

Figure 2.1: A graph representation of $1.253 - \phi + \phi^2$.

ory. A phase response function can be represented in any way that a general function $f : [0, 1] \rightarrow [-1, 1]$ can be, but important considerations to balance are the expressiveness of the representation and the ease with which the representation can be recombined and/or mutated. As demonstrated in [44] an incredibly expressive representation for a function like $f : [0, 1] \rightarrow [-1, 1]$ is to view the problem as one in symbolic regression, where the function is represented exactly as a closed form mathematical expression.

In particular it is possible to express the closed form mathematical equation for a function as a Directed Acyclic Graph where each node contains a mathematical operator. The graph is parsed recursively, where the value of a node that contains an operation is equal to the values of its children and its operation while nodes without children must be either constants or variables. For example, a node that contained the operation – is equal to value of its left child minus the value of its right child. Figure 2.1 displays the representation for $1.253-\phi+\phi^2$.

One clear advantage of this representation is that unlike discretization, symbolic regression always returns functions with continuous derivatives, especially important because many previous PCO results are dependent on first and second order derivatives [33, 50]. Furthermore, as discussed in [45] directed

acyclic graphs are well suited to reasonable crossover operators, and serve as a relatively modular representation.

Notice though that this symbolic regression representation is not able to represent function with a discrete number of discontinuities. In order to allow for phase response curves that are occasionally discontinuous during some runs we expressed the total function $f : [0, 1] \to [0, 1]$ as a collection of directed acyclic graphs each used on adjoining intervals of $[0, 1]$. Indeed, it will turn out the best phase response curves have a single discontinuity, and the GA discovers this regardless of whether exact discontinuities are allowed or must be approximated.

Crossover

The benefit in a GA from maintaining a population of potential solutions stems from the ability to combine old solutions to make new ones via a crossover operator. Since we used a directed acyclic graph representation for phase response curves, the crossover operator takes as input two directed acyclic graphs and must return a recombination of them. We implemented crossover by taking one of the original graphs and replacing a node at a level k with a subgraph also at level k from the other solution.

2.1.2 Fitness of a Phase Response Curve

In our setting the goal of a fitness function is to take a phase response curve and after extensive numerical simulation return a single score describing the abil-

ity of that phase response curve to synchronize. Described coarsely, we use a Monte Carlo sampling scheme augmented with some co-evolution [34]. Before considering the details of a fitness function for phase response curves it is worth considering what elements in a PCO system can affect the ability of the system to synchronize. Indeed, it is the case that in our framework all the elements of the system can affect whether the system synchronizes. Explicitly this means that changing the graph G, the time delay τ, the initial conditions, the oscillator frequencies and the phase response curves can either cause the system to synchronize or not. Ideally, our fitness function would be able to measure the ability of a phase response curve to reach synchrony across all possible graphs, system sizes, time delays and initial conditions, but this is of course not possible to do numerically. Instead, we must necessarily narrow the scope of fitness function, such that a computer only evaluates several discrete PCOs systems.

To accomplish this focus we restrict our attention to situations where the delay is fixed at a value $\tau < .5$, and consider only a single random graph model and sample from uniform random initial conditions. There are two real risks involved in restricting the fitness function to only Random Geometric Graphs (RGG). The first risk is that phase response curve that performs well on these graphs is specific only to random geometric graphs. However, as we later show in Chapters 3 and 4 there are analytic bounds that suggest this first risk in not particularly relevant. The second risk is that there might be phase response curves that perform very well on most graphs, but for some reason do not perform well on RGGs. This second risk is much harder to directly address, but even if it were true the structure in RGGs closely resembles the structure one would expect in a wireless sensor network, and thus such a bias would not be too bad for the intended application area. Indeed, it would be quite peculiar if

there existed a phase response curve that was guaranteed to reach synchrony on wireless sensor network graphs but did not perform well on RGGs.

Thus we use a fitness function which can be described by the vectors

$$< G_1, \cdots, G_R >,$$

$$< \Phi_1, \cdots, \Phi_R >,$$

$$< \Omega_1, \cdots, \Omega_R >$$

where a phase response curves is tested on R trials, where trial k involves integrating the PCO system for a fixed amount of time on a graph G_k, with initial phase conditions Φ_k and in runs where frequencies are allowed to differ, with frequencies Ω_k. Each trial is then scored based on the firing times in the last few time units in the following way: First, in order to weed out curves that cause Xeno like solutions, (where oscillators are nearly constantly excited and thus fire too frequently) PRC's that lead to frequencies that are too short are discarded. Second, to establish what time most resembles the synchronous solution, we simply scanned the last five time units to find a small window of time, (we used a window of size 0.10) during which the most oscillators fired. Given this window, we used several ways of scoring. The first way we scored the solutions was based solely on the number of oscillator that fired in the window. Alternatively, we used the mean squared error inside the window and assigned a penalty for each oscillator that failed to fire in the window. The final fitness is then taken simply as the mean score over the trials.

In order to prevent over-fitting the tuples (G_k, Φ_k, Ω_k) corresponding on which the phase response curves perform best are routinely discarded and replaced—consistent with a coevolution paradigm [34]. Interestingly, the results

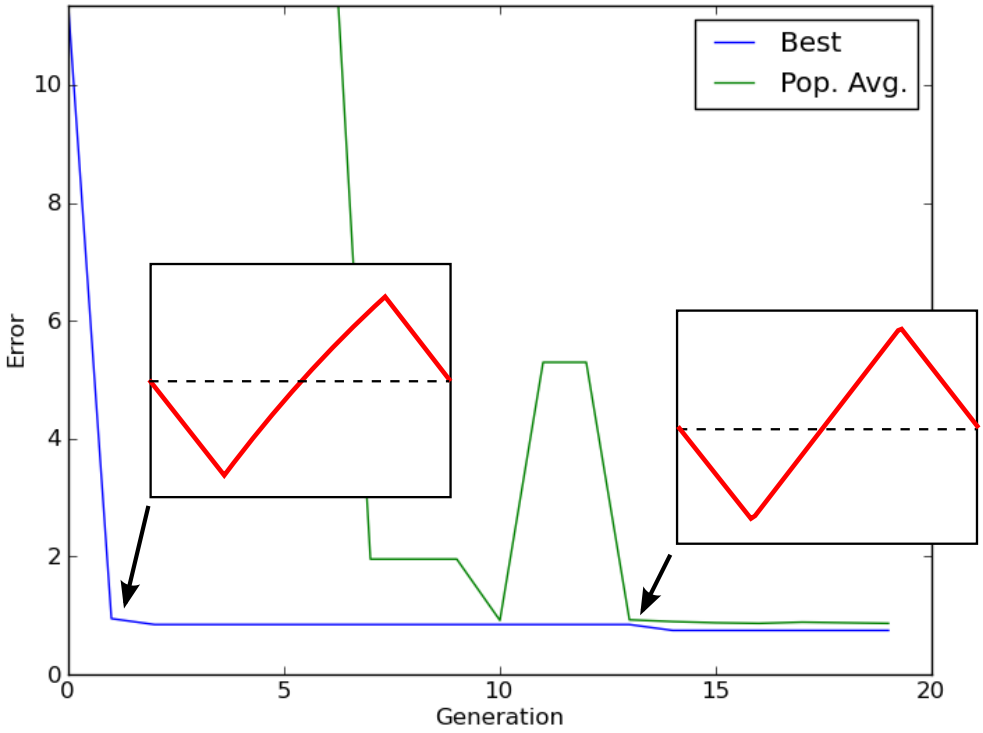

Figure 2.2: Without heterogenerities the GA converges quickly to low error values. Re-sampling of the graphs used for fitness calculations can lead to increases in some phase response curve errors.

we show do not seem to be particularly sensitive the choice of fitness function, with the caveat that it is very important to discard solutions that produce very large frequencies.

2.2 Results

Figure 2.2 displays the GA result when run on a random geometric graph with 400 nodes, with uniform time delay of 0.05 and homogeneous oscillators. Notice

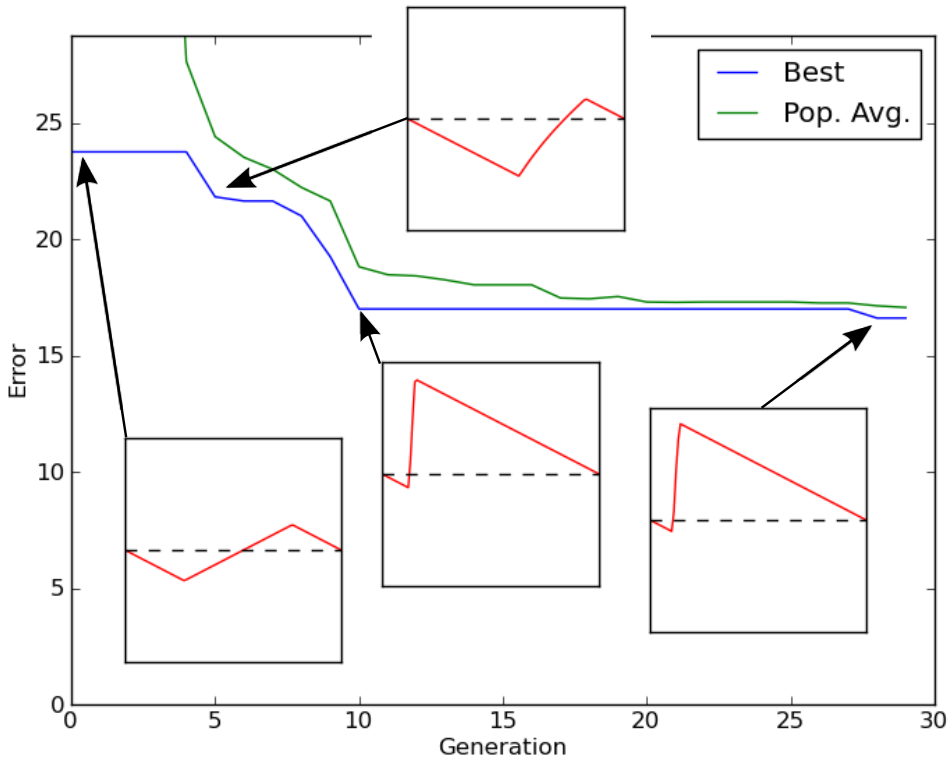

Figure 2.3: The solution of the genetic algorithm when run with heterogenous frequencies

that the GA almost immediately discovers a PRC that performs extremely well, and makes only minor adjustments thereafter. Indeed, it appears to be the case that on random geometric graphs learning PRC for homogeneous oscillators is relatively straightforward for our choice of function representation. Notice though that the resulting PRCs resemble curves recently studied in [54, 53] in that they are initially inhibitory and then later excitatory.

Learning a function that can deal with heterogeneities in frequencies requires more work. Figure 2.3 displays the solution produced from the GA optimization when run with a range of frequencies equal to 0.05, uniform delay,

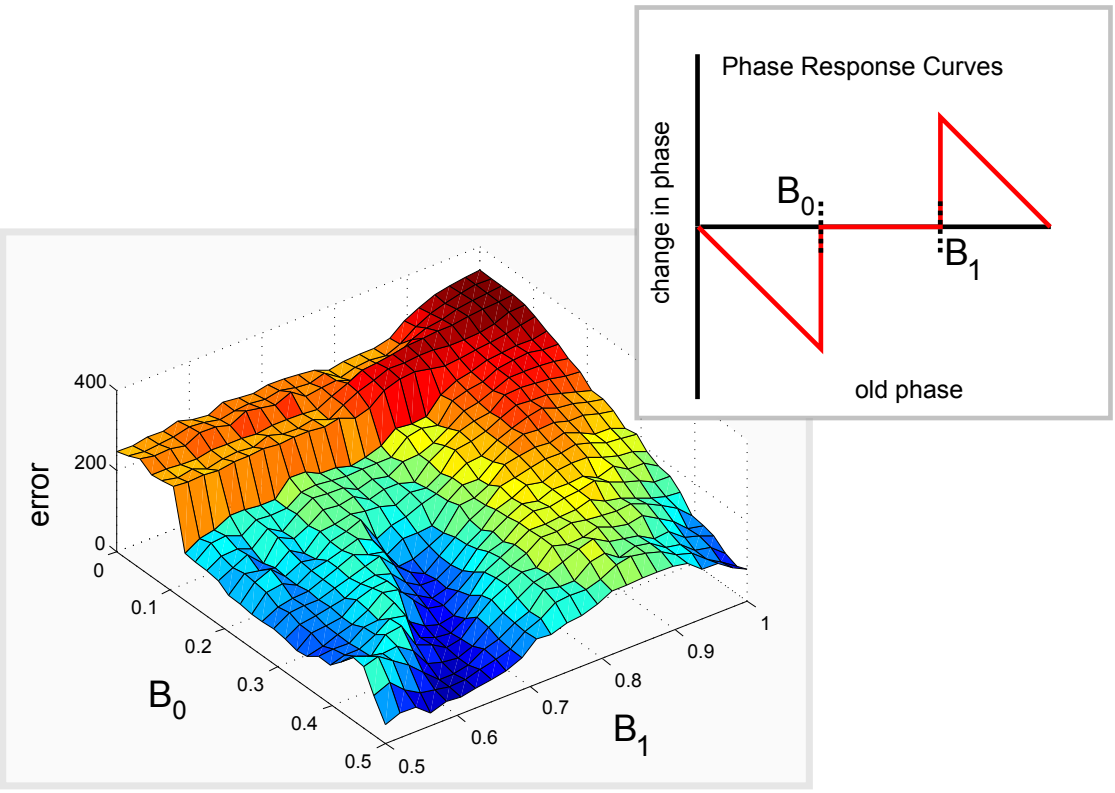

Figure 2.4: The error can be viewed as a function of the amount of inhibition and excitation in the phase response curve, where the curve is changed corresponding to the insert. Note that inhibition twice the time delay corresponds with a sharp decrease in the error while excitation reduces error but does so gradually. An error of 399 would imply that no two oscillators fire in the same time window. When $B_0 = 0$ and $B_1 = 1$ the corresponding phase response curve is constantly 0, implying no interactions between oscillators.

and processing delay of 0.05 on a random geometric graph with 225 nodes. In particular the GA quickly discovers once again the value of including both inhibition and excitation, and then slowly explores the tradeoff between when to switch between inhibition and excitaiton. The last optimal phase response curve is primarily excitatory, after a value slightly larger than the twice the time delay.

The relative error tradeoff between inhibition and excitation is further ex-

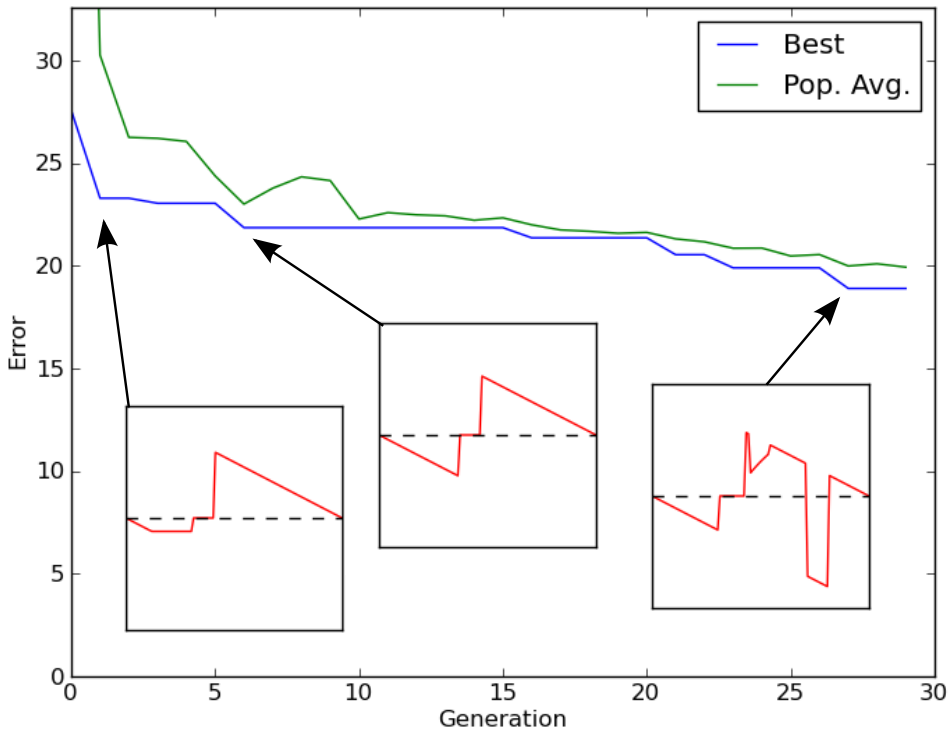

Figure 2.5: The solution of the genetic algorithm when run with heterogeneous oscillator frequencies and delays is still able to approach synchrony, but is more prone to over-fitting .

plored in 2.4, where it is seen, this time on a RGG with 400 nodes, that there is a critical value of inhibition at twice the time delay beyond which inhibition allows for a significant improvement in the system performance. Meanwhile, increasing excitation generally leads to better synchronization with the caveat, that for larger values of B_0 the system performs well with no excitation at all. Indeed, the two minima in 2.4 are studied analytically in chapters three and four, where they are referred to as belong to classes STII and Strong Resetting respectively. Increasing frequency heterogeneity produces a similar figure to 2.4 albeit with overall greater errors.

Moving to full heterogeneity, figure 2.5 displays the results from a GA run with the same parameters as 2.3 but with additional signal delays corresponding to geometric distance up to a max of 0.05. Notice again that the ending phase response curve initially contains inhibition that is followed by excitation, though inhibition is more heavily featured. As evidenced by the final phase response curve, in this more general setting the GA is more prone to over fitting phase response curves to particular graphs, even when the graphs are regularly changed.

2.3 Delay and Complex Topology Prevent Over-fitting

One of the advantages of the fitness function's generality is that it allows inspection into how the results of the genetic algorithm optimization change with parameters. Of particular interest are the changes in the optimal solution, where the returned solution experiences a discontinuous qualitative change. When these changes occur while moving a solution from the simplest most idealized system to more complicated realistic systems such bifurcations identify system elements whose absence can lead to oversimplification.

We thus consider the solutions that arise as the complicating factors of: complex topology, delay, and heterogeneous frequencies are added to the system sequentially. Recall that when complex topology and delay are already present, the solutions presented by the GA retain key features even with the inclusion of heterogeneous frequencies. However, when a system lacks either complex topology or delay there are clear, easily represented solutions that converge to

synchrony rapidly, but are fragile to the inclusion of either delay or complex topology. In addition to numerical experiments, this over-fitting can be understood analytically.

For very simplified systems the optimal solutions are immediately clear and determining them does not require using a GA. Case in point, when the system has no delay the optimal solution can reach synchrony no faster than using the maximally excitatory phase response curve:

$$f(\phi) = \begin{cases} 0 & : \phi = 0 \\ 1 - \phi & : \phi \in (0, 1] \end{cases} \tag{2.1}$$

In such a situation the first firing cascades across the entire graph, immediately causing all oscillators to fire, and henceforth synchronizing them.

However, notice that introducing even a small delay leads to a particularly pernicious non-synchronous solution where firing cascades go out of control, leading to a singularity in oscillator frequencies as $\tau \to 0$. For example, consider a pair of oscillators both connected to each other. The first time oscillator 1 fires causes 2 to fire time τ later which in turn will cause 1 to fire. Indeed, in such a situation the oscillators must have frequency at least $\frac{1}{2\tau}$ and can have much faster frequencies on more complicated graphs.

Similarly, when the systems is on the complete graph and $n > 2$ a maximally inhibitory phase response curve is able to synchronize the system. For example:

$$f(\phi) = \begin{cases} -\phi & : \phi = [0, 1) \\ 0 & : \phi = 1 \end{cases} \tag{2.2}$$

converges to exact synchrony in two time units. With this phase response curve it is easy to check that if several oscillators fired at time t, then at time $t + \tau$

all oscillators have phase 0 and thus the system is synchronized. If only one oscillator fired at time t then at time $t + \tau$ that oscillator will have phase less than or equal to τ and all other oscillators will have phase 0. In this case several oscillators will fire together in at least one time unit, leading to the first case.

Again though, this complete graph phase response curve is fragile once restrictions on the graph are loosened. For example, consider three nodes connected in a line. If the left and right most nodes have initial phases that differ and are more than τ greater than the middle node's phase, then the middle node will never fire, making synchronization impossible.

Moreover, since the representation of 2.1 and 2.2 are straightforward symbolically, they are particularly easy for a symbolic regression based GA to find, and we propose, also easy for human scientists. Thus, while more complicated solutions may also synchronize systems with no time delay and systems on the complete graph, many reasonable computer or human optimizations will overfit in such situations.

To contrast, systems which contain both delay and complex networks present enough of a challenge that neither purely inhibitory or purely excitatory solutions appear to be optimal. Instead, the genetic algorithm returns STII type solutions, which continue to be able to synchronize on the simpler systems, though they take somewhat longer than 2.1 and 2.2 to do so.

It is worth noting that there is a growing recognition that phase response curves that mix inhibition and excitation are increasingly important in overcoming delay and complicated networks [26, 24] following publication of [37].

Indeed, it is likely that the difficulty that delay and complicated network structure posed to earlier PCO studies was due to the prevalence of PCO models that were purely excitatory or inhibitory. But moreover, this work suggest that efforts to design optimal pulse coupled oscillator systems for real world applications should likely include both delay and complex network structure, and that efforts that lack one of these features will be less likely to generalize. This is particularly pressing given the number of recent efforts to create applicable sensor net protocols that lack one of these features.

2.4 Chapter Summary

Running a GA to search for optimal phase response curves reveals both the importance of mixing inhibition and excitation, and the importance of delay and complex topology to avoiding over-fitting. Indeed, the results provide strong numerical evidence that STII and SR phase response curves are not only extremely effective at causing oscillator systems to converge to synchrony, they are easy to learn. The following chapters develop an analytic theory to describe the success of these curves.

CHAPTER 3

ROBUST CONVERGENCE OF PULSE COUPLED OSCILLATORS

In this chapter we analyze an interesting class of PCOs for which one can prove robust convergence results on arbitrary aperiodic connected graphs, even with propagation delays and a non constant graph topology (such as when spatially embedded nodes are mobile). This class of PCOs is of particular biological relevance because it explicitly includes both inhibitory ("phase delay") and excitatory ("phase advance") regions in the phase response curve (PRC), much like the type II PRCs seen in nature [16, 46, 49, 18, 19, 3]. Additionally, these PCOs provide guidance for the design of engineered systems of PCOs; improving on the current technology by providing theoretical bounds for robust convergence under propagation delays and covering more diverse topologies.

Our analysis was motivated by the results of the previous chapter which used machine learning and genetic algorithms to engineer PRCs which would converge under propagation delays. In that chapter we found that such algorithms typically generate a very particular variety of type II PRCs. As we show below, for engineering applications such as sensor net synchronization [21, 27], these PRCs are superior to those typically used and allow for a precise analysis. Namely, our analysis does not rely on linear stability. Instead, we develop techniques that utilize the values of the PRC over the entire domain, not just the values of a derivative at a single point. The analysis also shows that precise normalization of inputs is not required to achieve synchronization with propa-

gation delays, unlike that suggested by the analysis in [50, 13].

3.1 Illustrative Examples

Before stating and proving the most general results, first we consider simplified phase response curves and sketch compelling arguments for these. For the sake of illustration, consider the PRCs we denote "strong reseting" (SR), where for some $B_0 \in (\tau, 1)$:

$$f_{SR}(\phi) = \begin{cases} -\phi & : \phi \in [0, B_0) \\ 0 & : \text{otherwise} \end{cases}$$

3.1.1 Synchrony is a Solution

Synchrony is clearly a solution for these curves; every oscillator is simply reset to 0 time τ after all oscillators fire. To study this solution consider the time $1 + \tau$ map, H.

$$H(\Phi(t_k)) = \Phi(t_{k+1}). \tag{3.1}$$

In general, the behavior of this map is very opaque. However, when phases are within a critical region detailed later, the convergence of $H(\Phi)$ to synchrony can be well understood.

3.1.2 Convergence of Strong Resetting Oscillators

There is also a clear way to understand the SR system near synchrony. Denote

$$\phi^+(t) = \max_i(\phi_i(t)),$$

$$\phi^-(t) = \min_i(\phi_i(t))$$

and

$$\rho(t) = \phi^+(t) - \phi^-(t).$$

Furthermore let

$$\rho_0(x, y) = \min(x - \tau, 1 - y + \tau),$$

where x and y are some system parameters. Then in the SR case, if at time t' no signals are en route and the range $\rho(t') < \rho_0(B_0, B_0)$, an analysis of the system shows that

$$H(\phi_i) = \min(\phi_i + \tau, \min_{j \in P(i)}(\phi_j)).$$

Namely, there are two cases that matter. In the first case i receives all its signals before it fires and thus does not adjust it phase, giving that $H(\phi_i) = \phi_i + \tau$. In the second case i receives a signal in its inhibitory region because there is a neighboring oscillator j with $\phi_j < \phi_i + \tau$ and thus ϕ_i is reset when the last signal reaches ϕ_i, leading to $H(\phi_i) = \min_{j \in P(i)}(\phi_j)$.

Notice that if an oscillator j succeeds an oscillator with phases ϕ^- then $H(\phi_j) = \phi^-$. In this way the minimum spreads, first to the successors of the minimum and then to the successors of the successors and so on. If the graph is aperiodic, then there exists some d such that d applications of the successor function, denoted: S^d, includes the whole graph. Thus on aperiodic graphs this process leads to synchronization.

3.1.3 Convergence of Strong Firing Oscillators

SR PRCs harness inhibition to stabilize synchrony, yet in many cases (such as when $\rho > .5$) excitation is useful, as it can allow an oscillator to push forward a cascade. It is possible to augment SR PRCs with excitation while preserving similar convergence bounds and methods of analysis, in the special case where the graph is undirected (directed aperiodic graphs are dealt with by a later theorem). Consider the PRC we denote "strong firing" (SF) where

$$f_{SF}(\phi) = \begin{cases} -\phi & : \phi \in [0, B_0) \\ 1 - \phi_i & : \text{otherwise} \end{cases}$$

Notice that in this situation oscillators always end up with phase 0 after they receive a signal, either by being reset or if the phase is greater than B_0, by firing.

To understand the map H in the SF case consider the excitation and inhibition separately, and again constrain $\rho(t') < \rho_0(B_0, B_0)$. It can be verified that between applications of H every oscillator fires. Let $\lambda_i(t_0)$ be the next time that i fires after some time t_0. During an application of H excitation leads to:

$$\lambda_i(t_0) = \min(t_0 + 1 - \phi_i(t_0), \min_{j \in P(i)} \lambda_j(t_0) + \tau).$$

Applying this map to an undirected graph implies that all oscillators fire within τ of their predecessors. The effect of the inhibition then behaves very similar to that of the SR case, where the relative phase differences are captured by

$$\min(-\lambda_i + \tau, \min_{j \in P(i)} - \lambda_j).$$

An interesting feature of the min map in the inhibition is that it preserves the τ predecessor-successor phase difference, which implies that after a single iteration of H the oscillators will no longer receive signals in the excitatory regime, leading to the same type of convergence as with SR PRCs.

3.2 Convergence of STII Oscillators

These two phase response curves converge because of the way a modified min map spreads across a graph, directed aperiodic in the case of SR and undirected aperiodic for SF. While the convergence of SR and SF PRCs is easy to understand other PRCs converge more robustly (as will be demonstrated later) and require a more general argument. Consider the family of PRCs, "strong type II" (STII) which have the following requirements. The first requirement is an initial "reset zone", $f_{ij}(\phi_i) = -\phi_i$ for $0 \leq \phi_i \leq \tau + \kappa$, where $\kappa > 0$. In addition the response curve must be slightly less than τ-inhibitory, in that $f_{ij}(\phi_i) \leq -\tau - \kappa$, on $[\tau, B_0]$ and then be excitatory, $f_{ij}(\phi_i) \geq 0$, for $\phi_i > B_1 \in [B_0, 1)$. An illustration of STII curves can be seen in Fig. 3.1. Notice that for phases in (B_0, B_1) there are no restrictions on f_{ij}, though the smaller this region is the larger the critical region will be. Similarly, it is not necessary that the PRC encode the value of τ in its shape, only that it is greater than τ inhibitory.

We can now generalize the results for the SF and SR PRCs to this new class. Furthermore this result remains true even if the graph changes over time. Indeed, suppose that the graph changes every $1 + \tau$ time, with graphs $G_1, G_2, \ldots G_k \ldots$. This leads to our main result: If each G_k has no isolated nodes, if there exists d such that $S_k(S_{k+1}(\ldots S_d(v)\ldots)) = V$ for an infinite number of k, and if the initial range $\rho < \min(B_0 - \tau, 1 - B_1 + \tau)$ the system will converge to synchrony (Notice that as τ approaches .5, B_0 and B_1 must approach 1). Furthermore if the previous conditions hold for all k then convergence occurs before time $t^* = \rho d / \min(\tau, \kappa)$. The graph conditions might at first seem onerous, but many such examples abound. For example, a grid that suffers a random edge

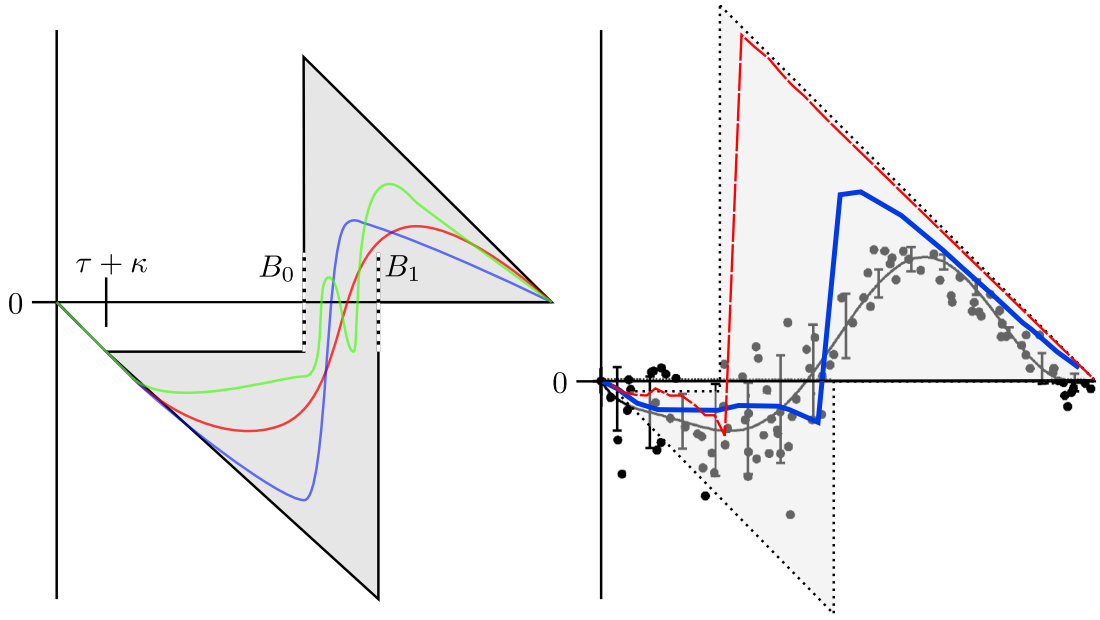

Figure 3.1: (Left) The value of τ and the shape of STII PRCs determine the values of B_0 and B_1 and thus the strength of the convergence results. (Right) Displayed are three different empirically generated PRCs, where the red dashed curve is from ventricular heart cell in an embryonic chick [19], the solid blue curve is from rabbit sinus node cells [3] and the data points with the line fit to them is from a low-threshold spiking GABAergic interneurons [49].

failure each time period would suffice, as would one where each G_k is a different random tree. Indeed, generic connected graphs are aperiodic, whereas periodicity is a special and fragile property. While the previous results for SF and SR PRCs were based on an understanding of how one phase spreads across the graph, this argument follows by focusing on the worst case sets of signals an individual oscillator can receive.

3.2.1 Oscillator Ranges Non-increasing

If initial conditions are contained in an interval of size ρ and there are no signals in transit, it is easy to see that this will remain true under iterations of the time $1 + \tau$ map. To see this, translate time so that the oscillators with the largest phase are just about to fire at time $t = 0$: $\phi^+(0^-) = 1$. The key insight is that all signals will occur within at most time $\rho + \tau$, since each oscillator can only fire once in that time, and any oscillator that has not fired will be in the excitatory region. In addition, note that the oscillator with the largest phase can not receive a signal until at least time τ so will always be inhibited by at least τ. Thus after time $1 + \tau$ it will be at most about to fire again, since it was inhibited at least τ and never excited. A careful analysis of the remaining oscillators using these insights shows that the time $1 + \tau$ map does not increase the size of the interval of phases and is given by the following lemma.

Lemma 3.2.1 *Given oscillators with phase response curves $f_i \in F$ and identical frequencies, uniform time delay and strongly connected graph, if at some t_0, $\rho(t_0) < \rho_0$ and no signals are enroute then, $\phi_-(t_0) \leq \phi_i(t_1) \leq \phi_+(t_0)$ for all i.*

In order to keep track of how many times an oscillator has fired since time t_0, consider a new phase variable,

$$x_i = \phi_i + p_i, \tag{3.2}$$

where p_i is the number of times that i has fired since t_0. By moving to this covering space this notation disambiguates subtraction and addition for oscillator phases (i.e. $1.1 - .9 = .2$). Let x^+ and x^- be the maximum and minimum phases.

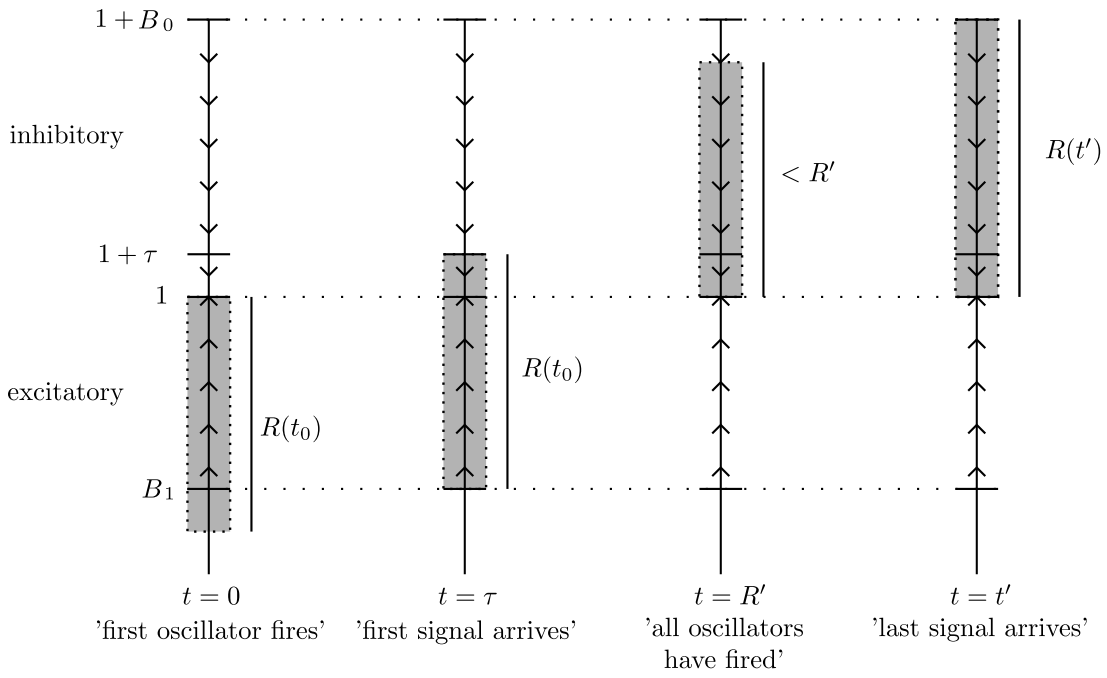

Figure 3.2: There are four key times during which the range of oscillators hits important milestones.

Since there are no signals enroute, without loss of generality translate time back by l, so that $x^+(0^-) = 1$ and $t_0 = -l$.

1: First it is shown that $\exists\, t'$ such that $x_i(t') \in [1, 1+\rho(0)+\tau]$ for all i. There are four important times to keep track of, displayed in figure 3.2.

Since $x^+(0) = 1 \Rightarrow x^-(0) = 1 - \rho(t_0)$ and since $\rho(t_0) > 1 - B_1 + \tau$, then $x_i(0) \geq x^-(0) > B_1 - \tau$ for any i. Thus, when the first possible signal arrives, at time τ, $x_i(\tau) > B_1$, which puts it in or past the excitatory portion of f. Thus all oscillators have fired by some time $\rho' \leq 1 - x^-(0) = \rho(t_0)$, and all signals from firings at 1 have arrived by $t' = \rho' + \tau \leq B_0$.

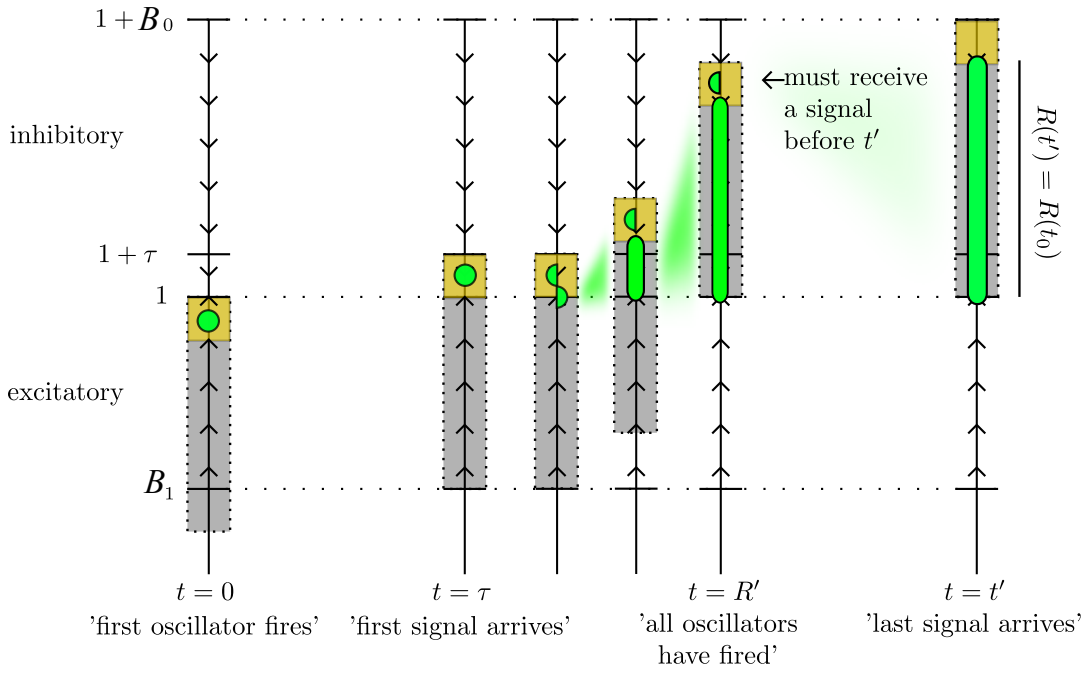

Figure 3.3: The range of possible locations of oscillators is separated into a two regions, the first colored yellow is of size τ. Oscillators with $\phi(0) < 1 - \tau$ can be excited to border of the yellow or inhibited towards the base of the range, but can never enter the yellow region.

Once an oscillator enters the inhibitory region, $[1, 1+B_0]$, it takes at least time B_0, before it can exit. Since $t' \leq B_0$, then after an oscillator fires at 1 it can only be inhibited. Thus, for any oscillator i, $x_i(t') \leq x_i(0) + t' \leq 1 + \rho' + \tau$.

Thus by t' all signals have been received and $x_i(t') \in [1, 1 + \rho' + \tau]$ for all i, implying that all oscillators have fired exactly once.

2: Next it is shown that at t', $x_i(t') \in [1, 1 + \rho']$ for all i.

Consider any oscillator i, let $\delta_i = x^+(0) - x_i(0)$. We consider two cases:

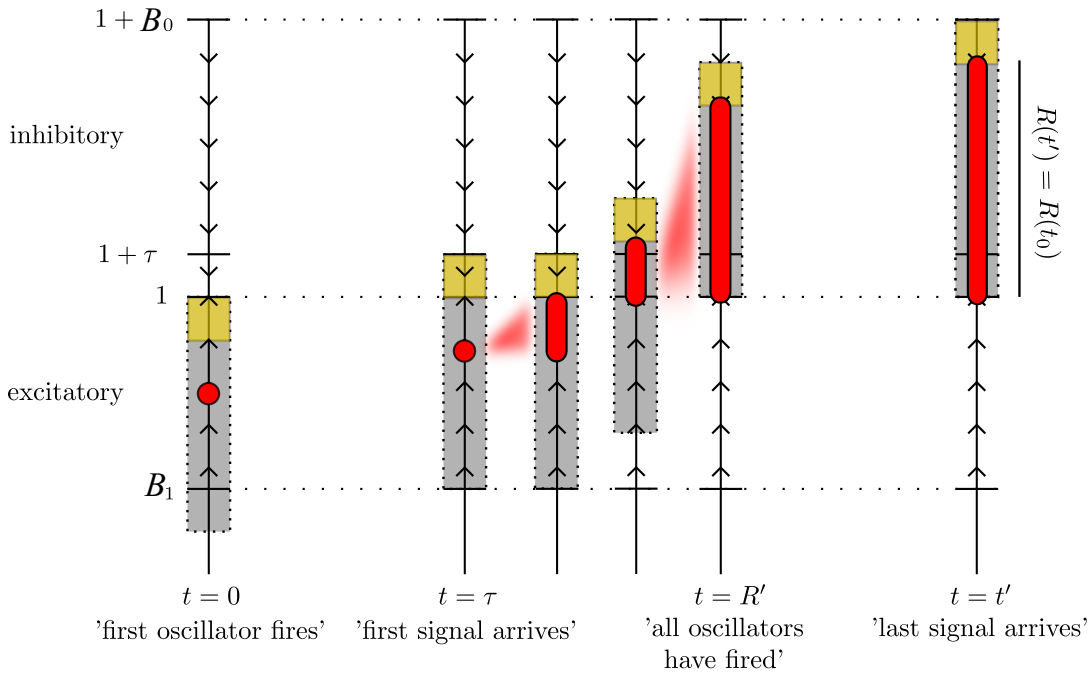

Figure 3.4: Oscillators beginning in the yellow region must eventually receive a signal, and thus be inhibited out of the yellow range.

1. If $\delta_i \geq \tau$, a signal can excite i but since no signal can arrive before time τ then $x_i(\tau) \leq 1$. Once an oscillator is in the inhibitory regime its phase is bounded by the time in the inhibitory regime giving: $x_i(t') \leq 1+t'-\tau = 1+\rho'$

2. If $\delta_i < \tau$, the first possible signal it can receive is at time τ, when $x_i(\tau) = 1 + \tau - \delta_i$, and thus it is in the inhibitory regime. Since $\min_{\phi \in [\tau-\delta, B_0]} f(\phi) = -\tau+\delta < 0$, and every oscillator receives a signal before t' (by strong connectedness) then:

$$\begin{aligned} x_i(t') &\leq (1 + \tau - \delta_i) + (t' - \tau) + (-\tau + \delta_i) \\ &= 1 + \rho' \end{aligned}$$

Thus at time t' there are no signals enroute and $x_i(t') \in [1, 1+\rho']$ for all i, giving that $\rho(t') \leq \rho' \leq \rho(0)$, and $\phi_i(t') \in [0, \rho']$ for all i.

3: Finally, it is shown that $\phi_i(t_1) \leq \phi_+(t_0)$ and $\phi_i(t_1) \geq \phi_-(t_0)$ for all i.

Since $x_i(t') \leq 1 + \rho'$ for all i and no signals are enroute at t', no oscillator can fire for at least time $1 - \rho'$. Recall that $1 + \tau = t' + 1 - \rho'$. Thus moving i forward in time from t' to $1 + \tau$ yields:

$$\begin{aligned} \phi_i(1+\tau) &\leq (1+\rho') + ((1+\tau) - t') \\ &= 1 \\ &= \phi_+(0). \end{aligned}$$

Recall that $\phi_+(-l) = \phi_+(t_0)$, then $\phi_i(t_1) \leq 1 - l = \phi_+(t_0)$. Similarly, since $\phi_i(t') \geq 0$ for all i then

$$\begin{aligned} \phi_i(1+\tau) &\geq (1+\tau) - t' \\ &= 1 - \rho' \\ &\geq \phi_-(0) \end{aligned}$$

giving that: $\phi_i(t_1) \geq 1 - \rho' - l \geq \phi_-(t_0)$. □

It's also possible to understand the previous accounting in a primarily graphical manner. Figure 3.2 displays the total range that all oscillators can possibly inhabit, showing the intermediary result that the total range cannot increase by more than τ from a single firing. Next, figures 3.4 and 3.3 follow an individual oscillator, showing that regardless of whether the oscillator begins in the first τ portion of the range, or not, that oscillator must eventually inhabit the gray region of the range.

3.2.2 Convergence on Aperiodic Graphs

As the previous subsection detailed, STII oscillators with phases inside the critical range ρ_0 will not diverge from each other. Now we show that the range of possible oscillator phases must also decrease.

Consider oscillators with $\phi_i(0) \leq 1 - \epsilon$ where $\epsilon = \min(\kappa, \tau)$. Such an oscillator will not fire until at least time ϵ. Now consider the successors of such an oscillator, j with $\phi_j(0) > 1 - \epsilon$. Oscillator j will receive a signal from i at $t > \epsilon + \tau$ when it is in inhibitory region, so will be inhibited by a sufficient amount such that $\phi_j(1 + \tau) \leq 1 - \epsilon$. A careful argument also shows that if $\phi_j(0) \leq 1 - \epsilon$ this will remain at time $t + \tau$. Iterating this argument d times (recall that S^d is the complete graph) on the oscillator with the smallest phase, shows that the time $d(1 + \tau)$ map will reduce the size of the phase interval by at least ϵ, or if it is less than ϵ the phases will completely synchronize. We formalize this argument in the following lemma and theorem.

Lemma 3.2.2 *For a system satisfying the hypotheses in 3.2.1, if at time t_k for some k there exists i such that: $\phi_+(t_k) - \phi_i(t_k) \geq \epsilon$ for $0 < \epsilon \leq \min(\kappa, \tau)$ then $\phi_+(t_k) - \phi_j(t_{k+1}) \geq \epsilon$ for all j in $S(i)$.*

Without loss of generality translate time back by l so that $t_{k-1} \leq 0 \leq t_k$ and $x^+(0) = 1$. Let $\delta_i = \phi_+(0) - \phi_i(0)$ and let s be the time when i fires. If i is excited by a signal before it fires, that signal can only arrive after time τ giving $s \geq \tau \geq \epsilon$. Otherwise, i will simply fire at time δ_i giving that $s \geq \epsilon$.

When i fires, it sends a signal that reaches each of its successors at time $s + \tau$.

For j in $S(i)$ two scenarios can occur when this signal arrives:

1. $x_j((s+\tau)^-) \in [B_1, 1+\tau+\kappa]$. In this case $x_j((s+\tau)^+) \leq 1$. This gives that by time $1+\tau$:

$$\begin{aligned} x_j(1+\tau) &\leq x_j(s+\tau) + ((1+\tau) - (s+\tau)) \\ &= 2 - s. \\ &\leq 2 - \epsilon. \end{aligned}$$

2. $x_j((s+\tau)^-) \in [1+\tau+\kappa, 1+B_0]$. Here $x_j((s+\tau)^+) \leq x_j((s+\tau)^-) - \tau - \kappa$, so:

$$\begin{aligned} x_j(1+\tau) &\leq x_j(s+\tau) + ((1+\tau) - (s+\tau)) \\ &\leq (s+\tau) - \tau - \kappa + ((1+\tau) - (s+\tau)) \\ &= 2 - \kappa \\ &\leq 2 - \epsilon. \end{aligned}$$

Thus $\phi_j(1+\tau) \leq 1 - \epsilon$ and $\phi_+(0) - \phi_j(1+\tau) \geq \epsilon$. Translating time back by l gives $\phi_+(t_{k-1}) - \phi_j(t_k) \geq \epsilon$. □

Notice that this previous lemma easily lends itself to a statement about all successor nodes under the following iteration.

Lemma 3.2.3 *For a system satisfying the hypotheses in 3.2.1, if at time t_k for some k there exists i such that: $\phi_+(t_k) - \phi_i(t_k) \geq \epsilon$ for $0 < \epsilon \leq \min(\kappa, \tau)$ then $\phi_+(t_k) - \phi_j(t_{k+m}) \geq \epsilon$ for all j in $S^m(i)$.*

Apply 3.2.2 m times. □

Repeated application of this lemma is enough to show the convergence of the system to synchrony on aperiodic graphs. For an aperiodic graph G let N be the number of iterations such that the successor function contains all nodes in G, or $S^N(v) = V$ for all $v \in V$ (Interestingly, there is a connection between this N and the Frobenius number, which characterizes the largest integer amount a set of coins in specific denominations cannot create [4]).

Theorem 3.2.4 *Given oscillators with phase response curve $f_i \in F$ and identical frequencies, uniform time delay and on a strongly connected aperiodic graph, if at any time t_0 there are no signals en-route and $\rho(t_0) \leq \rho_0$, then the system will converge to synchrony.*

Lemma 3.2.1 shows that $\rho(t_k)$ is a non increasing function with time steps t_k. Lemma 3.2.3 will be used to show that $\rho(t_k)$ is decreasing.

Applying lemma 3.2.3 to $\phi_-(t_k)$ yields:

$$\phi_+(t_k) - \phi_j(t_{k+N}) \geq \min(\rho(t_k), \kappa, \tau) \tag{3.3}$$

for all $j \in V$ giving that:

$$\phi_+(t_k) - \phi_+(t_{k+N}) \geq \min(\rho(t_k), \kappa, \tau). \tag{3.4}$$

Thus if $\rho(t_k) \leq \min(\kappa, \tau)$ then $\rho(t_{k+N}) = 0$ and the system is synchronized. Otherwise, if $\rho(t_k) > \min(\kappa, \tau)$ then $\rho(t_{k+N}) \leq \rho(t_k) - \min(\kappa, \tau)$. Thus after N time steps ρ is either zero or decreases by $\min(\kappa, \tau)$, giving that in $\lceil N\frac{\rho(t_k)}{\min(\kappa,\tau)} \rceil$ steps the system reaches synchrony. □

When the aperiodicity assumption is dropped, synchrony remains a solution, but is only neutrally stable. For example, if G is undirected, then G is either

aperiodic or bipartite. If G is bipartite, it has sets of vertices U and V such that $P(U) = V$ and $P(V) = U$. In this case the nodes of U synchronize with each other, while separately, the nodes of V synchronize with each other. More generally on periodic graphs the nodes on $P^n(i^+), P^{n+1}(i^+) \ldots P^{n+m}(i^+)$ may each independently synchronize.

3.2.3 Benefits of STII Oscillators

The benefit of the more general class of phase response curves can be seen in Fig. 3.5. In Fig. 3.5 the PRC "Limited Resetting", which has values strictly greater than $-.1$, is more likely to converge than SR PRCs when run on a slightly modified binary tree with uniform initial conditions. Indeed the combination of inhibition and cuts that divide a graph into multiple disjoint subgraphs can lead to solutions where nodes along the cut never fire (and where the phases are never smaller than the critical ρ). The risk of these non synchronous solutions increases with the amount of inhibition in the PRCs, the number of different disjoint subgraphs and the size of the cuts.

An important application of this result arises in sensor networks [21, 27, 22, 7, 14, 52, 9], that is, collections of many small sensors which communicate over radio frequencies. There has been great interest in the use of PCOs to provide a simple and robust mechanism to synchronize sensor networks. Such systems have intrinsic propagation and processing delays. In addition, most sensor networks have a complex graph structure, and a not necessarily constant network topology. However, most theoretical analyses ignore delays and assume the complete graph. As seen in Fig 3.6, these assumptions are quite significant.

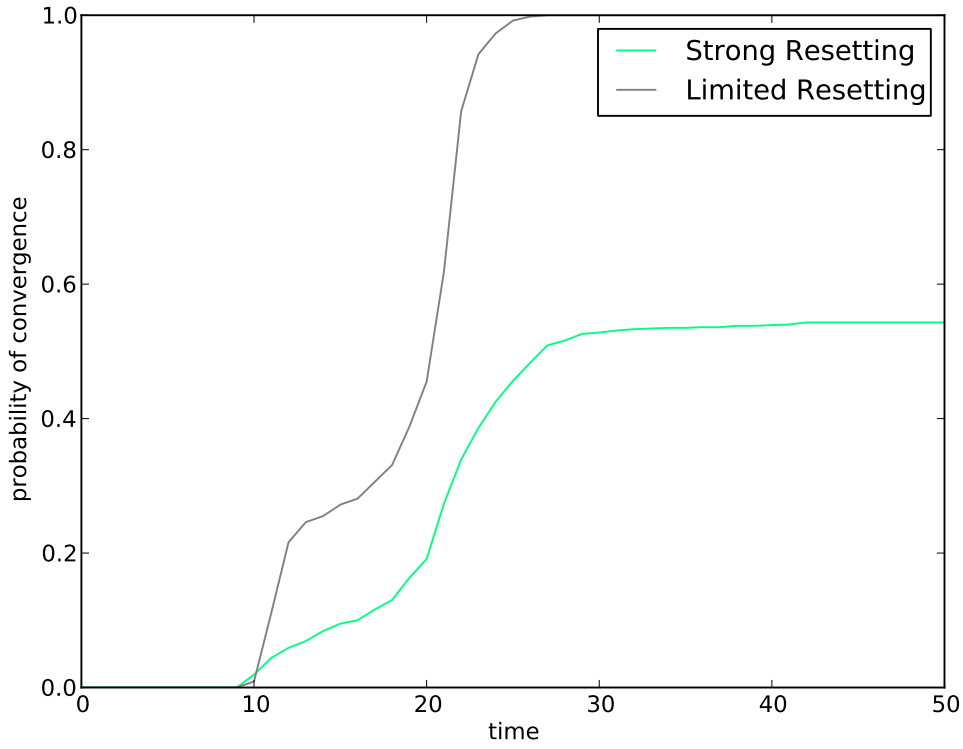

Figure 3.5: Limited Resetting offers more robust convergence on a binary tree with a single triangle and uniform random initial conditions than SF. (The 'S' like shape of the graph is due to whether the system converges to a phase on the same side of the tree as the triangle or far.)

In particular under the assumptions in our first result, the type II PRCs converge rapidly and robustly, while the currently most popular PRCs [21, 27] have bounded error but fail to synchronize exactly. In addition, even when we consider more realistic conditions, such as variations in propagation delay times and heterogeneous oscillator frequencies, the type II PRCs still perform well, while the top competitors do not.

Furthermore, the system is relatively robust to error. For example, Notice

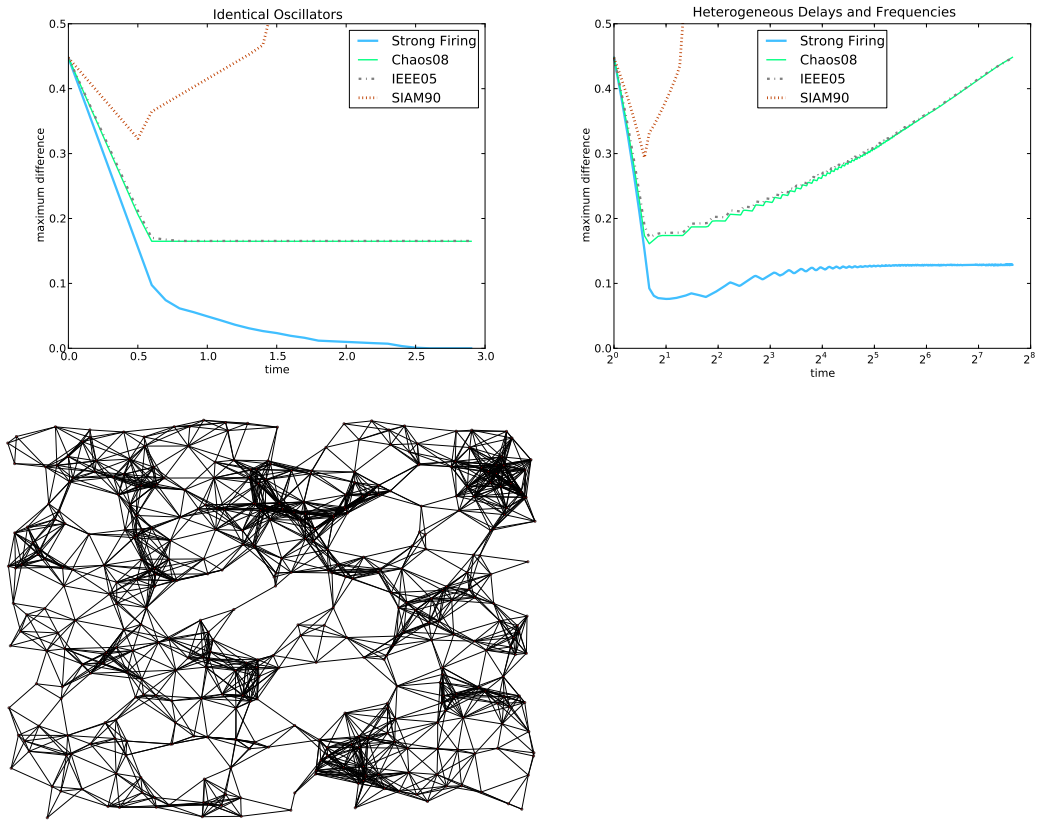

Figure 3.6: (a) Under the theoretical setting with a uniform delay of 5% STII curves outperform others from Chaos08 [27], IEEE05 [21], and SIAM90 [33] (b) This trend continues under more realistic settings, with frequency error up to 2.5% and transmission and processing delay also up to 2.5% (c) The random geometric graph on which these simulations was run. Data points are taken when oscillators are within a range of .5 and no signals are en route.

that the provable basin of attraction is the greatest when $B_0 = B_1 = .5 + \tau$, in which case the the system converges so long as $\rho < .5$. In this case, with probability 1 the synchronous solution is robust to any single random error in the oscillator phases.

Our detailed convergence analysis allows us to "tune" the PRCs for specific objectives. For example, as discussed in [27] in sensor-net applications it is im-

portant that the oscillators be allowed to "sleep" for as long as possible between firings. In our model this corresponds to choosing a large interval $[B_0, B_1]$ and setting the response curve to 0 in that region. However, choosing a large interval decreases the basin of attraction for the synchronous state. A simple and robust solution for this problem, would be to start with small interval $[B_0, B_1]$ and then expand it over time. For example, one could start with $B_0 = B_1 = 1/2 + \tau$ which allows for a large initial interval of phases and then reduce B_0 (and increase B_1) by τ or less every $2d(1 + \tau)$ units of time, stopping when $B_0 = 2\tau$. This provides provable convergence with a long sleep period outside of an initial period.

In the case where the delay τ is known in advance then the oscillators can simulate the arrival of their own signal to themselves τ time after they fire. This modification has the effect of adding self loops to the graphs, vastly increasing the kind of underlying sensor networks that this system performs well on. Indeed, if ever node has a self loop the only additional requirement on the graph is that the graph never becomes permanently unconnected.

Type II PRCs have also been seen in many places in nature [16, 46]. As seen in Fig. 3.1, actual phase response curves taken from cells in the heart and from some cortical interneurons are described by STII PRC suggesting that the stability of synchronous solutions in these settings may be described by our system. Furthermore, that this family of curves was discovered by a genetic algorithm [36] lends credence to both the evolability and the performance of such PRC for providing synchrony.

3.2.4 Convergence of STII Oscillators with Weights

Thus far the discussion has included only unweighted graphs, yet many biological graphs are weighted. Consider the extension which allows each edge's PRC to be weighted such that $f_{ij}(\phi) = -\phi$ for $\phi \leq w_{ij}$ and less than w_{ij} for $x \in [w_{ij}, B_0]$. Additional bookkeeping in the above proof allows one to show that a similar convergence follows with the added condition that $\Sigma_j w_{ij} > \tau$. Given the similarity of the proof for the weighted version, it is relegated to the appendix.

This weighted version can also be used to give interesting analytic results in the situation where we have some advance knowledge of the underlying graph topology. For example, if the indegree of the graph is known to be at least k, then the PRCs only need to be "resetting" over the interval from 0 to τ/k. This implies that in the limit of high indegree, the resetting region approaches the origin and the only requirement on the magnitude of the inhibition is that the PRC have a slope of -1 at the origin and be nonzero in the inhibitory domain.

One can also use high indegree to provide strong probabilistic convergence results. For example, for any STII PRC that is nonzero in the excitatory region there exists a constant c such that if the indegree of the connection graph is larger than $c \log(n/\epsilon)$ then under uniform random initial conditions the system will converge to synchrony with probability of at least ϵ. In general, for a well chosen STII phase response curve one can give explicit bounds on the probability of convergence for any non zero initial distribution of oscillator phases by analyzing the indegrees. This argument is extended and elucidated in the next chapter.

Other modifications are possible too. One such modification is the addition of "quiescent" period q, where oscillators ignore signals for time q after receiving a signal. This modification allows for a more general class of PRCs that are allowed more freedom between 0 and τ. This new system can be shown to converge on all strongly connected graphs, even periodic graphs and is discussed in the final chapter.

3.3 Chapter Summary

In summary, the family of STII phase response curves that was introduced is relatively general and includes curves that were empirically found in systems which synchronize in nature. Furthermore, we proved that this family of PCOs has a robust region in which it converges to synchrony on strongly connected aperiodic graphs. This convergence remains even in the presence of uniform time delay and particular mutations in the graph. It was then noted that in numerical trials this method outperforms similar PCO based time synchronization methods for wireless sensor networks. This advantage remained in numerical runs even when heterogeneous time delays, frequencies, and random errors were introduced.

CHAPTER 4

PROBABILISTIC CONVERGENCE BOUNDS

In this chapter we build upon the previous chapters, where we found that a class of Type II PRC, denoted "Stong Type II" or "STII", could consistently, (but not always) converge to synchrony on fairly complex graphs with time delays, and would approximate synchrony even with delay and frequency heterogeneity [37]. This convergence was explained by showing that these PCOs would converge to synchrony if their phases were inside a critical range ρ_0, essentially showing an l^∞ ball of stability. This showed that with well-tuned parameters the system is robust to any individual oscillator error or a combination of small errors; explaining the possibility of synchrony, but not the ubiquity of it in numerical simulations. For example, if the critical range is $\frac{1}{2}$ of the phase interval, then the probability that a system of n oscillators with uniform random initial conditions starts in the critical regime is $\left(\frac{1}{2}\right)^n$, which is exponentially small in the system size; however, numerical experiments show that convergence is in fact highly likely and our analysis explains this.

In particular, we use network analysis to expand on the local understanding of stability, using node indegrees to create a lower bound on the probability of random initial conditions converging to the critical region in any size system (finite or infinite).

This analysis of STII oscillators sheds light on some of the natural questions regarding Type II phase response curves, and the contribution of excitation and inhibition to synchronization in Type II PRCs. For example, it's clear that the important aspect of the excitatory end of a Type II phase response curve is that it allows for firing cascades, yet previous analytic results have tended to focus on the importance of inhibition when the system has time delays [37, 50]. In contrast the result in this chapter classifies the excitation in a type II PRC into different discrete classes, each class corresponding to its ability to cascade and a lower bound on the probability convergence.

As in the previous chapter we first describe the approach for a simplified phase response curve and reserve the detailed analysis for the later, more general theorem.

4.1 Bounds for Strong Firing Oscillators

To demonstrate the ability of STII oscillators to reach synchrony on complex graphs with time delays, consider Figure 4.1, which shows the maximum differences between oscillator phases as a system is integrated for different PRCs and random initial conditions. Notice that not only are STII curves the only curves that converge, but for most runs (computational trials) STII curves fall within the critical range in a single unit of time, despite the fact that the size of the critical range is exponentially small in probability space. As will be shown, a large portion of the basin of attraction of synchrony in STII oscillators can be described by this rapid convergence to the critical range. Furthermore, this con-

vergence to the critical range arises from a fundamentally different mechanism, and relies on different properties of the PRC than the convergence inside the critical range.

To understand this basin analytically, consider first, the most extreme STII PRC, the "strong firing" (SF) PRC introduced in the previous section. Recall:

$$f^{SF}(x) = \begin{cases} -x & : \phi \in [0, B) \\ 1 - x & : \phi \geq B \end{cases}.$$

Notice, the response f^{SF} gives to any signal causes an oscillator to have phase 0, where signals received after B also cause it to fire. This brief characterization of the SF PRC allows for a quick analytic description of one way in which the SF PRC converges rapidly to the critical range as described in the next section.

4.1.1 Union Bound

To get a bound on the probability of convergence we reduce the behavior of this dynamical system into a combinatorial question which can be addressed by utilizing the union bound. The key insight is that if every SF oscillator i receives a signal or fires in a small window of time (denoted as event E_i for each oscillator i) then every oscillator will be reset to phase 0; thus all phases will be within the critical range (note: the first firing in a complete graph always satisfies this condition, and thus the complete graph will always converge). We will show that the window can be as large as $1 - s$, where

$$s = \max(B, 1 - B + 2\tau).$$

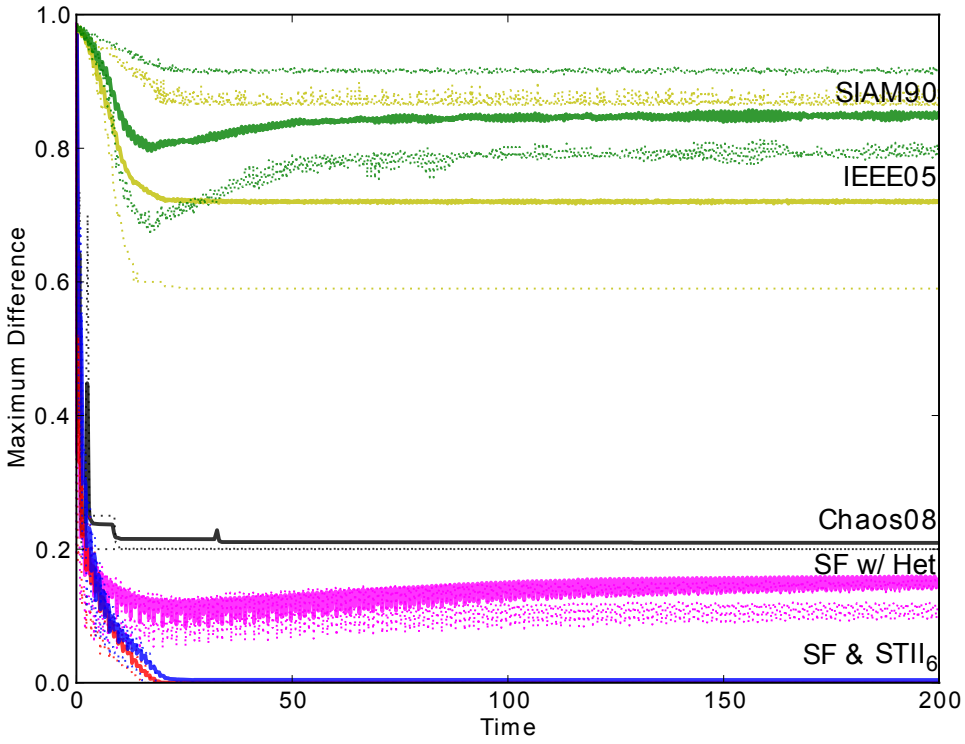

Figure 4.1: Starting from uniform random initial conditions in a system with 400 nodes, trajectories (mean – solid line, middle 50% – between dotted lines) either converge to synchrony or not depending on the PRC. Notice that SF and STII oscillators converge to exact synchrony in finite time while others from Chaos08 [27], IEEE05 [21], and SIAM90 [33] do not (this remains true in other measures). When the same systems have heterogeneous frequencies and heterogeneous delays synchrony is no longer a solution, but the SF PRC can approximate it as shown in curve 'SF w/ Het' (Also true for STII curves, not shown).

Notice, that if every oscillator receives a signal or fires at some time in $[\tau, 1-s+\tau]$, then for all i,

$$\phi_i(1 - s + \tau) \leq 1 - s \leq B - 2\tau.$$

Since only oscillators with phases greater than B can generate signals, no new signals are being sent. Thus by time τ later all signals will have arrived at their destinations, giving that for all i,

$$\phi_i(1 - s + 2\tau) \leq 1 - s + \tau \leq \rho_0$$

which puts all oscillators in the critical range with no signals enroute.

Therefore, the probability that the SF system converges can be bounded by the likelihood that every oscillator receives a signal in a window of size $1 - s$ time, $P(\cap_i^n E_i)$, which can then be bounded by using node degrees, d_i. If at time 0, $\phi_j(0) \in [s, 1]$ then all the successors of j will necessarily receive a signal in time $[\tau, 1-s+\tau]$ (since $s \geq B$, j is in the excitatory regime) and if $\phi_j(0) \in [s-\tau, 1-\tau]$ then j must fire in $[\tau, 1 - s + \tau]$. (Note: that this is now very similar to the probability that a random subset of the graph will dominate it, connecting it to some sensor net protocols used to find a Connected Dominating Set [23, 8] and the study of dominating sets in general [6]). Thus, for uniform random initial conditions a simple bound on the probability of any oscillator i receiving a signal or firing in $[\tau, 1 - s + \tau]$, is simply the complement of all i's predecessors having phases in $[0, s)$ and $\phi_i \in [0, s - \tau] \cup [1 - \tau, 1]$; yielding

$$P(E_i) \geq 1 - s^{d_i+1}.$$

Notice, that the probability of a node i failing to receive a signal in the $1 - s$ time window is exponentially small in that node's indegree. These probabilities

can be aggregated using the Union Bound, giving that:

$$P(\cup_i^n E_i^c) \leq \Sigma_i^n s^{d_i+1}$$

and thus

$$P(\cap_i^n E_i) \geq 1 - \Sigma_i^n s^{d_i+1}.$$

Alternatively, a slightly stronger bound can be found using the fact that each E_i is positively correlated, or that the number of nodes dominated is a submodular function of node subsets (as detailed for the more general case later), giving the probability of convergence:

$$P_{SF}(G) \geq P(\cap_i^n E_i) \geq \Pi_i^n (1 - s^{d_i+1}). \tag{4.1}$$

Thus the deterministic bound from [37] has been used to create a statement about convergence from random initial conditions for a system of any size n.

4.1.2 Bounds for Random Graphs

This probabilistic bound immediately gives a number of interesting corollaries. For example, let $\delta_n(p)$ be the minimum indegree such that the $P_{SF}(G) > p$ then solving (4.1) for node degrees leads to:

$$\delta_n(p) \ \leq \ln(1-p)/\ln(s) - \ln(n)/\ln(s),$$

which is logarithmic in the system size. To give a sense of the constants, the minimum value for s occurs when $B = s = .5 + \tau$, and thus to ensure a 95% convergence rate in a systems with a time delay 5% of the period:

$$\delta_n(0.95) \leq 5.02 + 1.68 \ln(n);$$

a result that holds for any n.

This result can also be used to make statements about the convergence of SF oscillators on random graphs. Take an Erdős-Rényi random graph, $G(n, \hat{p})$, where edges are created with independent probability $\hat{p}$. In this case an application of Chernoff's inequality shows that if

$$\hat{p} \geq \frac{\ln(n)}{n} g(s, \gamma)$$

for a function g of s and $\gamma << 1$ then as $n \to \infty$, the probability of synchrony

$$P_{SF}(G) \to (1 - 1/n)e^{1/n^{1-\gamma}} \to 1.$$

Notice, that this requirement on $\hat{p}$ is only a constant multiple of that required for $G(n, \hat{p})$ to be connected, which asymptotically, occurs when

$$\hat{p} \geq (1 + \epsilon)\frac{\ln n}{n}.$$

Thus, the degree requirements grow reasonably with n, and furthermore, since convergence requires connectedness, our rigorous bound is a constant factor approximation of the actual required degree.

Similarly, one can show asymptotic bounds on random geometric graphs, constructed by positioning nodes uniformly at random on the unit $\bar{d}$ dimensional torus and connecting any nodes within some radius r. If r is chosen so that the expected degree

$$r^{\bar{d}} n\theta = c \ln(n),$$

(where θ is the volume of a $\bar{d}$ dimensional unit ball) then utilizing results describing the minimum degree in random geometric graphs, [40] shows that the system will converge to synchrony as $n \to \infty$ so long as c is the greater of the

solutions to:

$$\frac{1}{c} = 1 + \frac{2}{c \ln s} - \frac{2}{c \ln s} \ln(\frac{-2}{c \ln s}).$$

Again, a constant factor of logarithmic growth in the expected degree gives probabilistic convergence guarantees.

As with the two previous examples, (4.1) can be used as a tool to turn degree bounds into PCO convergence bounds. In particular, any bound on the minimum degree of a network (finite or infinite) can be turned into a bound on the probability of PCOs with random initial conditions converging on that network.

Of course in many situations results for finite n are more relevant than asymptotic guarantees. Figure 4.2 displays the analytic lower bound for P_{SF} for several Random Geometric Graphs, and how this bound increases with increasing edge densities.

4.1.3 Computational Analytic Bounds

For situations where precise estimates of $P_{SF}(G)$ are important one can use a computational analytic approach by running multiple single time step Monte Carlo trials and checking if the phases fall within the critical range. In a graph with m edges such a routine can be implemented by an event based simulation, and thus can run in $O(m \log m)$ time. Whereas typically integration time scales with system size, our analytic bound shows that this computational analytic routine remains viable as the system size increases. Such numerical routines have thus far shown that while convergence is particularly impeded by low degree structures such as rings or stars, random networks converge better than

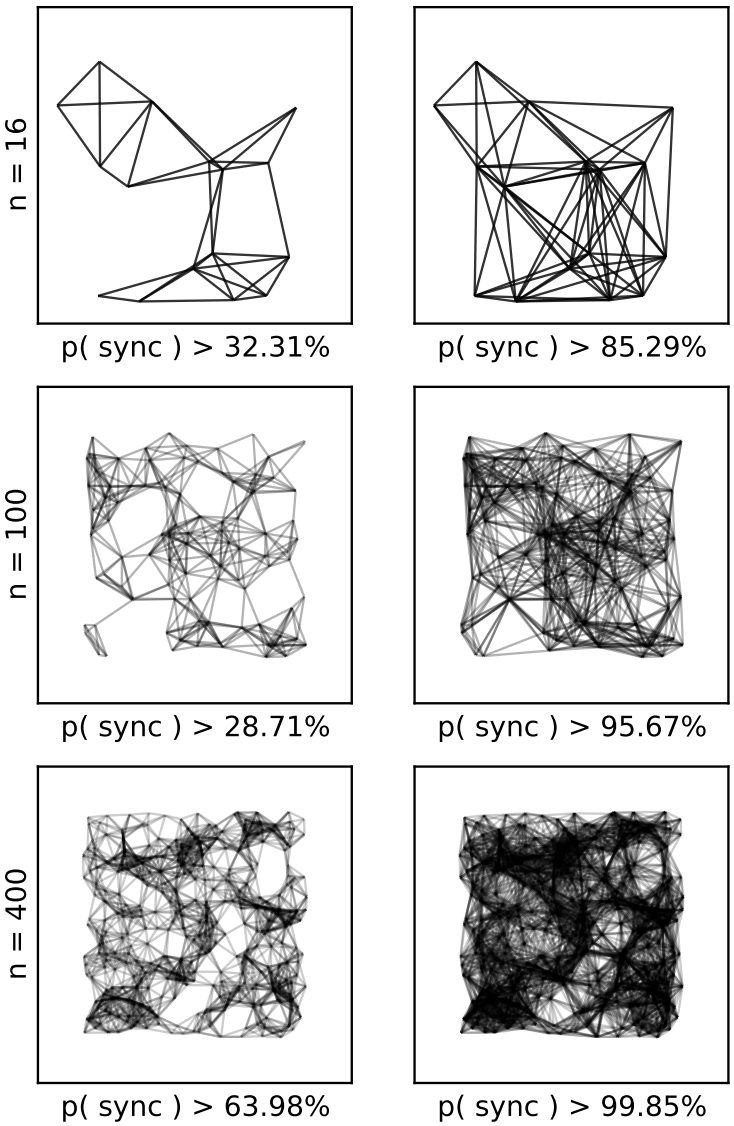

Figure 4.2: The computed lower bound for the convergence of pulse coupled SF oscillators on random geometric graphs at several finite sized systems, once for networks with low degrees and again with higher degrees.

our worst case analytic bound.

4.2 Bounds Based on Phase Response Curve Shapes

We now consider more general PRCs, showing that many STII PRCs will also have

$$\delta_n(p) = O(\log(n))$$

and thus will also have corresponding probabilistic guarantees for random graph models and rigorous computational routines. The key feature of the SF PRC was that a single signal causes an oscillator to reset or fire. The arguments made for an SF oscillator can be modified to allow for oscillators that require multiple signals to reset or fire.

4.2.1 New Framework for PRCs

Consider the sub class $STII_{k,\eta}$ which, as opposed to requiring 1 signal, will require receiving at least k signals within $1 - s - \eta$ time in order to emulate the response of an SF oscillator. For simplicity, we furthermore restrict $STII_{k,\eta}$ so that $B_0 = B_1 = B$, implying that these curves are strictly inhibitory before they are strictly excitatory.

Determining if a phase response curve is a member of $STII_{k,\eta}$ involves two steps: first, classifying the strength of the inhibitory section, and second, the strength of the excitation. We say that an oscillator i is h-inhibitory if receiving

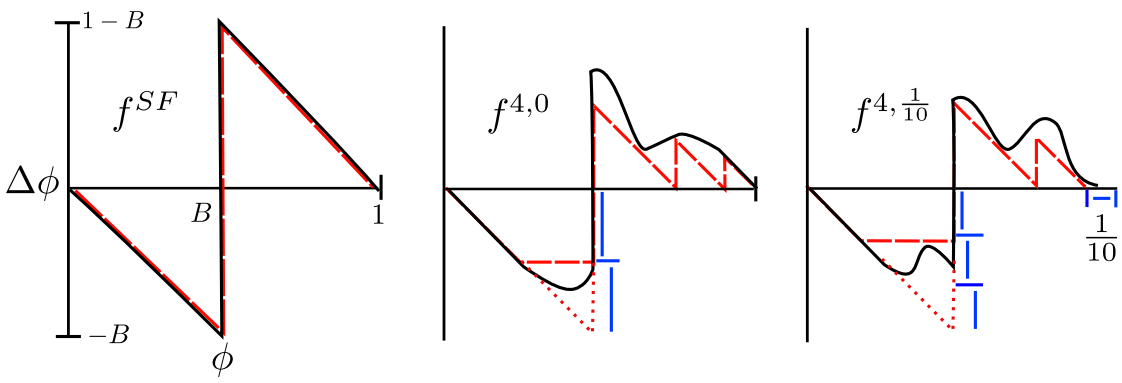

Figure 4.3: (Color online) Placing a sawtooth function underneath the excitatory portion of an $STII$ PRC provides an upper bound on the number of excitations that will cause the oscillator to fire. A curve's inhibition is measured in proportion to B.

h signals in the inhibitory region over some span of time $[t_0, t_0 + s']$,

$$s' = 1 - s - \eta$$

forces $\phi_i(t_0 + s') < s'$. Similarly, an oscillator i is $(k - h + 1)$-excitatory if receiving $k-h+1$ signals in the excitatory region, in some time $[t_0, t_0+s']$, forces an oscillator to fire before $t_0 + s' + \eta$. As seen in figure 4.3, a sufficient condition for $(k - h + 1)$-excitability is that the PRC is greater than a saw tooth with slope -1 when $x \in [B, 1 - \eta]$. If an oscillator is both h-inhibitory and $(k - h + 1)$-excitatory then it is a member of $STII_{k,\eta}$.

4.2.2 A Probabilistic Lower Bound

Based off this generalization of the phase response curves, one can use similar methods as before combined with Chernoff's inequality to bound the probability of the system synchronizing.

Lemma 4.2.1 *For a system of oscillators in $STII_{k,\eta}$, if at time t every oscillator i either has at least k neighbors j, each with $\phi_j(t) \in [s+\eta, 1]$ or $\phi_i \in [s-\tau, 1-\tau]$ then at time $t+1-s+2\tau$ all oscillators are within the critical range ρ_0 and no signals are en route.*

Without loss of generality translate time so that $t = 0$. First consider an oscillator i that neighbors k oscillators with $\phi_j(0) \in [s+\eta, 1]$. Since $s \geq B$, any oscillator j with $\phi_j(0) \in [s+\eta, 1]$ is in the excitatory regime. Thus, j must fire sometime in $[0, 1-s]$, creating a signal that reaches its neighbors τ time later. Since i has at least k neighbors with $\phi(0) \in [s, 1]$, then i will receive at least k signals sometime in $[\tau, 1-s+\tau]$, causing that oscillator to be excited to firing, inhibited to 0 or receive total inhibition equal to $-B$. Thus,

$$\phi_i(1-s+\tau) \in [0, 1-s].$$

Meanwhile, if an oscillator i has $\phi_i \in [s-\tau, 1-\tau]$ then i is in the excitatory regime by the time the first signal arrives at time $t = \tau$ and will thus fire before time s , implying $\phi_i(1-s+\tau) \in [0, 1-s]$

Next we show that the restriction that $s = \max B, 1-B+2\tau$ gives that these oscillators with phases in $\phi(1-s+\tau) \in [0, 1-s]$ are in the inhibitory section of the phase response curve. If $s = B$ then $B \geq 1-B+2\tau$ and thus $-B \leq -\frac{1}{2}-\tau$. Thus $1-s = 1-B \leq \frac{1}{2}-\tau \leq B-2\tau$. Similarly, if $s = 1-B+2\tau$ then $1-s = B-2\tau$. Since $1-s < B-2\tau$ then all oscillators are in the inhibitory regime, and will remain so for τ time regardless of any signals.

Thus at time $1-s+2\tau$ no signals will be en route and $\phi_i(1-s+2\tau) \in [0, 1-s+\tau]$. Since $s = \max(B, 1-B+2\tau)$ then $1-s+\tau \leq \rho_0$ and all oscillators are therefore within the critical range. □

In the following two lemmas let a forthcoming oscillator refer to an oscillator i which at time t either has $\phi_i \in [s-\tau, 1-\tau]$ or has at least k neighbors such that each neighbor j has $\phi_j(t) \in [s+\eta, 1]$. Furthermore, for a distribution ζ let $\int_s^1 \zeta(x)dx = q$ and $\int_{s-\tau}^{1-\tau} \zeta(x)dx = q_0$.

Lemma 4.2.2 *If oscillator phases are drawn independently from distribution ζ, the probability a node i with degree d_i is forthcoming is at least*

$$1-(1-q_0)e^{\frac{(qd_i-k)^2}{2qd_i}}.$$

The probability that an oscillator i has less than k neighbors ready to fire is the sum of the binomial distribution $X \sim B(d_i, q)$ from 0 to $k-1$. Chernoff's inequality [35] states that this probability can be bounded by

$$P[X < (1-\delta)\mu] < e^{\frac{-\mu\delta^2}{2}}.$$

Choosing $\delta = 1 - \frac{k}{qd_i}$ yields the bound that the probability that i has less than k neighbors ready to fire is less than $e^{-\frac{(qd_i-k)^2}{2qd_i}}$. Thus either i has k neighbors almost ready to fire or is in the excitatory regime itself with probability $1-(1-q_0)e^{\frac{(qd_i-k)^2}{2qd_i}}$.
□

Lemma 4.2.3 *If graph G has node degrees $d_1, d_2, ..., d_n$ and at time t oscillator phases are drawn independently from distribution ζ then the probability that each node is forthcoming is greater than $\Pi_{i=0}^{n} 1-(1-q_0)e^{\frac{(qd_i-k)^2}{2qd_i}}$.*

Let E_i denote the event that at time t, oscillator i is forthcoming. Lemma 4.2.2 gives the value of $P(E_i)$ as $1-(1-q_0)e^{\frac{(qd_i-k)^2}{2qd_i}}$. Notice that since E_i depends on only

$\phi_j(t)$ for $j \in N(i)$ and $j = i$ then E_i is uncorrelated with with any E_k for $k \notin N(i)$. Indeed, for event E_i to occur it must be that for some $j \in N(i)$, $\phi_j(t) \in [s, 1]$ and thus all events E_k for $k \in N(j)$ are more likely to occur. Thus all E_I are either uncorrelated or positively correlated, and the probability that E_i occurs for all i is greater than

$$\Pi_{i=0}^{n} P[E_i] = \Pi_{i=0}^{n} 1 - (1 - q_0) e^{\frac{(qd_i - k)^2}{2qd_i}}$$

□

The following theorem is then immediate.

Theorem 4.2.4 *For independent initial conditions, on a strongly connected aperiodic graph G with degrees d_i and phase response curves $f_{ij} \in F_{k,\eta}$, then the probability of convergence is given by:*

$$P_{f_{k,\eta}}(G) \geq \Pi_{i=1}^{n} 1 - (1 - q_0) e^{\frac{(qd_i - k)^2}{2qd_i}}. \tag{4.2}$$

Alternatively the union bound can give a lower bound of

$$P_{f_{k,\eta}}(G) \geq 1 - \sum_{i=1}^{n} (1 - q_0) e^{\frac{(qd_i - k)^2}{2qd_i}}.$$

In this case let

$$c_n = \ln(n) - \ln(1 - p),$$

then the system will converge with at least probability p if for all i, the expected number of firing neighbors,

$$d_i q \geq k + c_n + \sqrt{c_n^2 + k c_n}.$$

Since, for fixed k this result also scales $O(\ln(n))$ then the random graph results in the SF case have analogous results of the same order: $\hat{p} = O(\frac{\ln(n)}{n})$ for Erdős-Rényi and $r = O(\frac{\ln(n)}{n^{1/d}})$ for random geometric graphs.

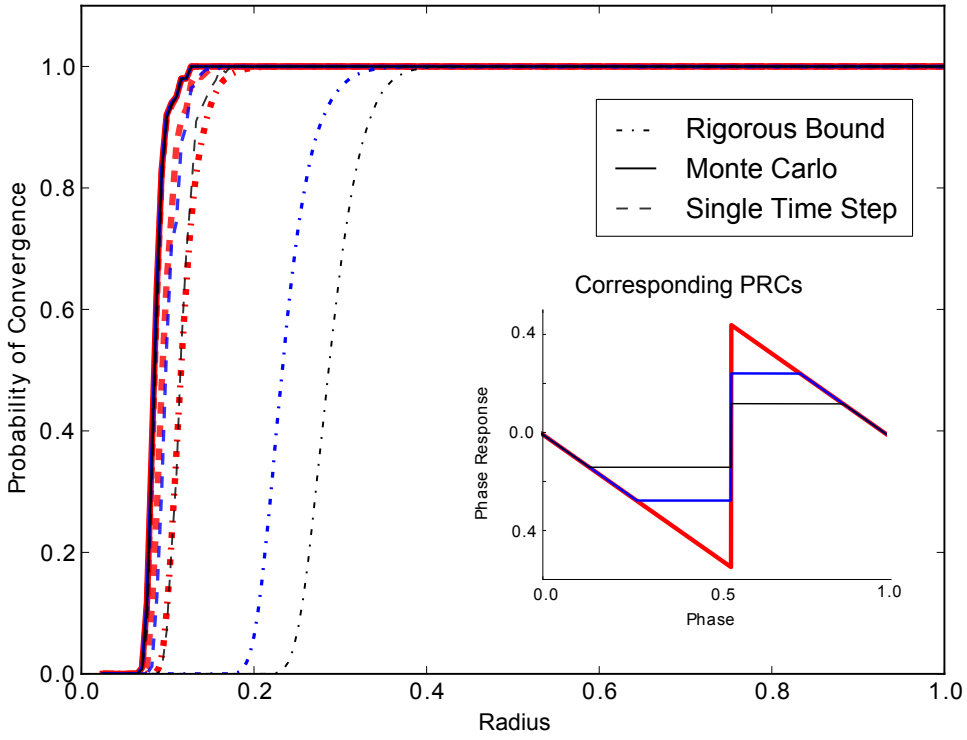

Figure 4.4: (Color online) Probability of convergence for a 400 node random geometric graph as a function of radius for SF (red/thick), $STII_{4,0}$ (blue) and a $STII_{7,0}$ (black/thin) PCOs. Numerical results (solid) suggest that all three oscillators systems transition to synchrony at the same value of r. Dotted lines show an analytic lower bound and dashed lines show the numerical single time step bound.

These results can also be used to prove a bound for the performance of a similar rigorous computational routine. The performance of a $STII_{7,0}$ and a $STII_{4,0}$ as well as their probabilistic guarantees can be seen in figure 4.4.

A Bound for Weighted Systems

Finally, it is worth noting that in many systems, such as systems of neurons, edges are often weighted and the impact that different neighbors have varies drastically [50]. The results in this paper also extend to a weighted version, where each edge has weight w_{ij} and weights are interpreted by the formula: $\hat{f}_{ij}(x) = \max(-w_{ij}, f_{ij})$ for $x < B$ and $f_{ij}(x) = \min(w_{ij}, f_{ij})$ for $x > B$, where w_{ij} acts as a constraint of the phase response curve. The above formula for the $P_f(G)$ remains true so long as for each i, $\sum_j w_{j,i} \geq \tau$ and for each node i there are d_i nodes j such that $f_{ij} \in F_{h,k}$.

In such a case, if k increases as $O(\ln(n))$ or less then so does $\delta_n(p)$. Furthermore, if $k \to \infty$ then the requirements on the phase response curve shrink to simply requiring that $f'(0) = -1$, and $f(x) < 0$ for $x < B$ and $f(x) > 0$ for $x > B$ and that f is continuous everywhere except B where $\lim_{x \to B^-} < -\epsilon$ and $\lim_{x \to B^+} > \epsilon$. Thus for very large systems our results show convergence for a very general class of type II oscillators. However, when comparing to results for "weakly coupled oscillators" one should recall the slightly different requirement, that in those cases, $\sum_i w_{ij} = \epsilon$ and the weights are multiplicative: $f_{ij}(\phi) = w_{ij} f(\phi)$.

4.3 Non-Synchronous Solutions

Another way to understand the basin of convergence is to consider solutions other than synchrony. Namely, the existence of other solutions and their stability gives an upper bound on the basin of synchrony. In [37] we noted that for

STII PRCs at least one nonsynchronous solution will be present if the graph is structured so that there is a set of nodes whose removal splits the graph into at least three disjoint components and each of the removed nodes borders at least three of these components. The nonsynchronous solution had the property that each of the components were individually synchronized, but communication between these components was impossible as the cutting set was persistently inhibited and thus never never fired.

As shown in the previous chapter a binary tree can become entrained in a nonsynchronous solution. For a phase response curve of type $f_{k,\eta}$ this peculiar solution can occur if there is set whose removal divides the graph into $\frac{2k}{B}$ components, where each node in the set, neighbors at least one node in each component.

As before a balanced $\lceil 2\frac{k}{B} \rceil$ary tree is one such network structure. Indeed, one can even give a rough lower bound for the likelihood of this solution existing. Removing any of the nodes one level above the leaves divides the graph into $\frac{k}{B_0}$ components. For any node i one level above the leaves, i will not fire if $\phi_i(0)$ is in $[0, \frac{B}{2} - \tau]$, at least k of it's neighbors have phases in $[1, 1 - \frac{B}{2}]$, and i has another k neighbors in each bin of size $\frac{B}{2}$. The probability that each component only has phases inside a given bin of size $\frac{B}{2}$ gives:

$$P[\text{async}] \geq (\frac{B}{2})^n$$

While this probability may be exponentially small, it is sufficient to rule out proofs for global, or A.E. convergence.

It's worth noting that it has been shown in [26] that the presence of these non-synchronous solutions may be overcome by including stochastic elements,

such as random signal error. Indeed, if signals have a probability of never being received, eventually every oscillator will fire, simply because at sometime every oscillator will observe a time of length 1 without receiving any signals.

4.4 Summary

In summary, in this chapter we have shown how the local convergence of STII pulse coupled oscillators to synchrony can be extended probabilistically, relating graph density and phase response curve structure to a rigorous lower bound on the probability of convergence. Applying this lower bound to random graph models shows that the expected node degree beyond which synchronization is very likely is a constant multiple of the percolation threshold. Therefore a computational scheme that merely samples after the first $1 + \tau$ time is a constant factor approximation to a sampling routine that integrated for infinite time. An extension with edge weights was also discussed.

CHAPTER 5

CONCLUSIONS

Before concluding, it's worthwhile to once again consider synchrony framed loosely and broadly. We began this thesis by observing the empirical fact that decentralized coordination can be fascinating—at least to the visitors of the Great Smoky Mountain National Park and in the case of the synchronization of fireflies. Yet, given the full range of modern spectacle available to the average park goer, how is it that the simple coordination of fireflies remains impressive? Perhaps it is the simplicity of synchrony's description that allows it to hold such symbolic power for its observers—that synchronization represents a notion of 'agreement', or possibly that it stands as a proxy for the emergence of a singular entity from a collection of disparate parts. And to the eye, the process of synchronization may appear as a conflict, between the already synchronized and the soon to be or between different synchronous groups vying for dominance. In such a process is it more accurate to describe the process in terms of information being communicated across the system, or information being destroyed as the initial conditions are replaced with uniformity? Surely then, an imaginative park goer may see the synchronization of fireflies as something more than the peculiar behavior of a species of insect—and such a park goer would be justified in seeing past the particularities.

Indeed, these metaphors for synchronization can be more-or-less instantiated in wireless sensor network applications. Applying pulse coupled oscillator synchronization to wireless sensor networks is an application which utilizes synchronization as a method to reach agreement across the all the sensor network motes. It is also an application where notions of information are impor-

tant, and minimizing the required communication between motes is an explicit goal. And while in sensor networks the process of synchronization may not be a conflict between motes, failure to synchronize can destroy the functionality of the sensor network.

This strikes upon one of the benefit of studying synchronization. Synchronization is a general behavior, and studying it for fireflies, or neurons, or sensor nets advances our understanding in all its settings. Thus, searching for better pulse coupled oscillators for the synchronization of wireless sensor network not only has the prospect of increasing sensor accuracies, extending battery life and boosting broadcasting capabilities, it reveals at a fundamental level what kinds of synchronization are possible, and what qualitative design features aid synchronization. Yet ironically, while it is the simplicity of synchrony's description that allows for it's ubiquity, understanding it requires significant work.

Consequently, the goal of Chapter Two: designing new pulse coupled oscillators for wireless sensor networks, was achieved only after utilizing modern machine learning approaches. This new computer aided approach opened up a whole new possible line of inquiry, which resulted in strong new results for a specific pulse coupled oscillator system as well as informed clear overarching design criteria for pulse coupled oscillators more broadly.

First, the genetic algorithm we used suggested that a class of oscillators STII and SR phase response curves converge well and are easy to learn. Additionally, we found strong evidence that to avoid overfitting both delay and complex network topology are critical features to include in the system. Thus, by the end of Chapter Two our numerical approaches had both focused the relevant design

question, and suggested a potential answer, the STII oscillator.

Building on the results of Chapter Two, Chapter Three borrowed techniques and thinking from computer science to prove analytic convergence results for STII oscillators. Not only do these results go beyond standard linear stability results, they show explicitly how the overall shape of the STII phase response curve impact these convergence results. As such the analytic results in Chapter Two provide strong justifications for the importance of having inhibition, but limiting it to the beginning of the phase response curve—a critical qualitative design feature. Additionally, these results were generalized, showing that there is a natural generalization to systems with weights, a feature critical in a number of oscillator settings.

Finally, Chapter Four utilized techniques from network science to demonstrate analytic lower bounds on the probability of synchronization for STII oscillators. This result reveals a fundamental connection between synchronization and graph topology, giving bounds for synchronization phase transitions of the same asymptotic order as percolation on a number of random graph models. Moreover, while Chapter Three demonstrated the importance of initial inhibition in phase response curves, the work in Chapter Four demonstrated the fundamental importance of excitation in the design of phase response curves.

Taken as a whole this thesis has developed a new pulse coupled oscillator system with analytic guarantees to converge with high probability on many graphs. Not only is this system useful for the synchronization of wireless sensor networks its analysis has revealed several critical design features useful for the study of pulse coupled oscillator broadly. First, it has shown the importance

of including both delay and complex network topology to prevent overfitting pulse coupled oscillators. Secondly, the analysis of STII oscillators has revealed the importance of switching from an initial inhibitory region to an excitatory one for a system of pulse coupled oscillator. Lastly, we have demonstrated the power of analysis techniques from computer science and network science in answering dynamical system questions when typical dynamical system techniques are not applicable. Hopefully these lessons will inform the future studies.

5.1 Future Work

Finally, it is worth discussing potential future research in this area. As I see it, there are several key directions worth highlighting.

For instance, it may be possible to augment pulse coupled oscillators so that they can change their frequencies and thereby converge to synchrony even when oscillators begin with heterogeneous frequencies. Subsequently, it will be important to determine if such systems are particularly fragile to heterogeneous delays, and if so how best to deal with those. Indeed, finding ways to deal with oscillator heterogeneities will likely require adding a number of creative features to pulse coupled oscillators. One possible approach maybe the addition of limited memory, such as a 'quiescent' period or continued investigation of spontaneous signal errors suggested in [25, 24].

Additionally, it's possible that there are some theorems that provide information based bounds on pulse coupled oscillator synchronization. Indeed,

since synchronization fundamentally involves communication it may be possible to discern bounds on the amount of information that must be communicated to break the symmetries required for synchronization.

Finally, there is important work to be done in taking the abstract pulse coupled oscillator models and implementing them in circuitry. Indeed, such real world implementation typically requires considering additional constraints. There are some preliminary reasons to suspect that the PRCs that synchronize the best in the abstract model require adjustments in order to be easily represented in an analog circuit, in which case a number of interesting trade offs will have to be navigated.

In any case, future work will continue to determine what is, and is not possible in regards to the most basic coordination problem: synchronization.

APPENDIX A

APPENDIX FOR CHAPTER 3

A.1 Proof for Convergence on Weighted Graphs

Below we construct the more general versions of the lemmas and theorems in Chapter 3. While the vast majority of the proofs are similar, there is slightly more book keeping involved.

Lemma A.1.1 *Given oscillators with phase response curves $f_{ij} \in F(w_{ij})$ and identical frequencies, uniform time delay and strongly connected graph where $\Sigma_j w_{ij} \geq \tau$, if at some t_0, $\rho(t_0) < \rho_0$ and no signals are enroute then there exists time $t' < t_0 + \rho(t_0) + \tau$ such that $x_i(t') \in [1, 1 + \rho(0) + \tau]$ for all i.*

Since there are no signals enroute, without loss of generality translate time by l, so that $x_+(0) = 1$ and $t_0 = -l$.

As before there are four important times to keep track of: when the first signal is sent, when the first signal arrives, when all oscillators must have fired and when all signals must have arrived.

Since $x_+(0) = 1 \Rightarrow x_-(0) = 1 - \rho(t_0)$ and since $\rho(t_0) < 1 - B_1 + \tau$, then $x_i(0) \geq x_-(0) > B_1 - \tau$ for any i. Thus, when the first possible signal arrives, at time τ, $x_i(\tau) > B_1$, which puts it in or past the excitatory portion of f_{ij}. Thus all oscillators have fired by some time $\rho' \leq 1 - x_-(0) = \rho(t_0)$, and all signals from firings at 1 have arrived by $t' = \rho' + \tau \leq B_0$.

Once an oscillator enters the inhibitory region, $[1, 1+B_0]$, it takes at least time B_0, before it can exit. Since $t' \leq B_0$, then after an oscillator fires at 1 it can only be inhibited. Thus, for any oscillator i, $x_i(t') \leq x_i(0) + t' \leq 1 + \rho' + \tau$.

Thus by t' all signals have been received and $x_i(t') \in [1, 1 + \rho' + \tau]$ for all i, implying that all oscillators have fired exactly once and all those signals have arrived. Translating time back by l gives the desired result □

The next lemma will strictly improve this result.

Lemma A.1.2 *For a system under the hypotheses of A.1.1, if at some t_0, $\rho(t_0) < \rho_0$ and no signals are enroute then, $\phi_-(t_0) \leq \phi_i(t_1) \leq \phi_+(t_0)$ for all i.*

Again, without loss of generality translate time back by l, so that $x_+(0) = 1$ and $t_0 = -l$.

From lemma A.1.1 it is clear that any oscillator i will receive signals from all it's predecessors before time $\rho(t_0) + \tau$. Consider two cases separately.

First, examine the case where i receives any signal when $x_i(t) \leq 1$ or i is set back to 1 at anytime. Since no oscillator fires until time 0 and it takes time τ for a signal to reach it's destination then it must be that $x_i(s) = 1$ for $s \geq \tau$. Since i can only be inhibited past time s it must be that $x_i(\rho(t_0) + \tau) \leq \rho(t_0)$.

The only remaining situation to consider is when all the signals i receives are when $x_i > 1$, and none of them push i back to 1. Since by lemma A.1.1 every oscillator fires, and since i is never reset to 1 then it must be that i is set back by at

least an amount $\Sigma_j w_{ij} + \kappa$. Thus by time $\rho(t_0) + \tau$, $x(\rho(t_0) + \tau) \leq \rho(t_0) + \tau - \tau\Sigma_j w_{ij} + \kappa \leq \rho(t_0)$.

Since in either of these cases $x_i(\rho(t_0) + \tau) \in [0, \rho(t_0)]$ and there are no signals enroute then $x_i(t_1) \in [1 - \rho(t_0), 2]$. Translating time back by l gives the desired result. □

We next show a constraint on how an oscillator's phase affects its neighbors. Namely phases different from the maximal phase cause their neighbors to be different from the maximal phase.

Lemma A.1.3 *For a system satisfying the hypotheses in A.1.2, if at time t_k for some k there exists i such that: $\phi_+(t_k) - \phi_i(t_k) \geq \epsilon$ for $0 < \epsilon \leq \min(\kappa, \tau)$ then $\phi_+(t_k) - \phi_j(t_{k+1}) \geq \epsilon$ for all $j \in S(i)$.*

Without loss of generality translate time back by l so that $t_{k-1} \leq 0 \leq t_k$ and $x_+(0) = 1$. Let $\delta_i = \phi_+(0) - \phi_i(0)$ and let s be the time when i fires. If i is excited by a signal before it fires, that signal can only arrive after time τ giving $s \geq \tau \geq \epsilon$. Otherwise, i will simply fire at time δ_i giving that $s \geq \epsilon$.

Now consider oscillator $j \in S(i)$. Recall from the proof of A.1.2 that either $x_j(t) = 1$ at some $t \geq \tau$ or j receives at least inhibition $\Sigma_k w_{jk} + \kappa$. Notice that in the second case j receives inhibition at least $\Sigma_k w_{jk} + \kappa$, giving:

$$\begin{aligned} x(R + \tau) &\leq 1 + R + \tau - \Sigma_k w_{jk} - \kappa && \text{(A.1)} \\ &\leq 1 + R - \kappa && \text{(A.2)} \\ &\leq 1 + R - \epsilon && \text{(A.3)} \end{aligned}$$

giving the desired result. This leaves only the first case, where $x_j(t) = 1$ for some $t \geq \tau$, which is further broken down to two cases.

Consider first the case where not only is j at some point reset to zero, but that the signal from i does so, such that $x((s+\tau)^+) = 1$. In this case,

$$\begin{aligned} x((R+\tau)) &\leq x((s+\tau)^+) + (R+\tau) - (s+\tau) && \text{(A.4)} \\ &= 1 + R - s && \text{(A.5)} \\ &\leq 1 + R - \epsilon && \text{(A.6)} \end{aligned}$$

Finally consider the case where $x(t) = 1$ for $t \geq \tau$ but the signal from i doesn't reset j. For the signal from i to not reset j it must be that that signal instead inhibits j by at least $w_{ij} + \kappa$. Thus

$$\begin{aligned} x((R+\tau)) &\leq 1 + (R+\tau) - (\tau) - w_{ij} - \kappa && \text{(A.7)} \\ &= 1 + R - w_{ij} - \kappa && \text{(A.8)} \\ &\leq 1 + R - \epsilon && \text{(A.9)} \end{aligned}$$

Thus $\phi_j(1+\tau) \leq 1 - \epsilon$ and $\phi_+(0) - \phi_j(1+\tau) \geq \epsilon$. Translating time back by l gives $\phi_+(t_{k-1}) - \phi_j(t_k) \geq \epsilon$. □

Notice that this previous lemma easily lends itself to a statement about all successor nodes under the following iteration.

Lemma A.1.4 *For a system satisfying the hypotheses in A.1.2, if at time t_k for some k there exists i such that: $\phi_+(t_k) - \phi_i(t_k) \geq \epsilon$ for $0 < \epsilon \leq \min(\kappa, \tau)$ then $\phi_+(t_k) - \phi_j(t_{k+m}) \geq \epsilon$ for all j in $S^m(i)$.*

Apply A.1.3 m times. □

Repeated application of this lemma is enough to show the convergence of the system to synchrony on aperiodic graphs. For an aperiodic graph G let N be the number of iterations such that the successor function contains all nodes in G, or $S^N(v) = V$ for all $v \in V$.

Theorem A.1.5 *Given oscillators with phase response curve $f_{ij} \in F(w_{ij})$ and identical frequencies, uniform time delay and on a strongly connected aperiodic graph where $\Sigma_j w_{ij} \geq \tau$, if at any time t_0 there are no signals en-route and $\rho(t_0) \leq \rho_0$, then the system will converge to synchrony.*

Lemma A.1.2 shows that $\rho(t_k)$ is a non increasing function with time steps t_k. Lemma A.1.4 will be used to show that $\rho(t_k)$ is decreasing.

Applying lemma A.1.4 to $\phi_-(t_k)$ yields:

$$\phi_+(t_k) - \phi_j(t_{k+N}) \geq \min(\rho(t_k), \kappa, \tau) \tag{A.10}$$

for all $j \in V$ giving that:

$$\phi_+(t_k) - \phi_+(t_{k+N}) \geq \min(\rho(t_k), \kappa, \tau). \tag{A.11}$$

Thus if $\rho(t_k) \leq \min(\kappa, \tau)$ then $\rho(t_{k+N}) = 0$ and the system is synchronized. Otherwise, if $\rho(t_k) > \min(\kappa, \tau)$ then $\rho(t_{k+N}) \leq \rho(t_k) - \min(\kappa, \tau)$. Thus after N time steps R is either zero or decreases by $\min(\kappa, \tau)$, giving that in $\lceil N \frac{\rho(t_k)}{\min(\kappa,\tau)} \rceil$ steps the system reaches synchrony. □

BIBLIOGRAPHY

[1] *Synchronous fireflies*. `http://www.nps.gov/grsm/naturescience/fireflies.htm`, May 2013.

[2] A. ABOUZEID AND B. ERMENTROUT, *Type-ii phase resetting curve is optimal for stochastic synchrony*, Phys. Rev. E, 80 (2009), p. 011911.

[3] J. M. ANUMONWO, M. DELMAR, A. VINET, D. C. MICHAELS, AND J. JALIFE, *Phase resetting and entrainment of pacemaker activity in single sinus nodal cells*, Circulation Research, 68 (1991), pp. 1138–1153.

[4] M. BECK AND S. ROBINS, *Computing the continuous discretely: Integer-point enumeration in polyhedra*, Springer Science+ Business Media, 2007.

[5] C. C. CANAVIER AND S. ACHUTHAN, *Phase resetting and entrainment of pacemaker activity in single sinus nodal cells*, Math. Biosci., 226 (2010), pp. 77–96.

[6] M. CHELLALI, O. FAVARON, A. HANSBERG, AND L. VOLKMANN, *k-domination and k-independence in graphs: A survey*, Graphs and Combinatorics, 28 (2012), pp. 1–55.

[7] A. L. CHRISTENSEN, R. O'GRADY, AND M. DORIGO, *From fireflies to fault-tolerant swarms of robots*, IEEE T. Evolut. Comput., 13 (2009), pp. 754–767.

[8] F. DAI AND J. WU, *On constructing k-connected k-dominating set in wireless networks*, in Parallel and Distributed Processing Symposium, 2005. Proceedings. 19th IEEE International, april 2005, p. 81a.

[9] K. DENG AND Z. LIU, *Distributed computation of averages over wireless sensor networks through synchronization of data-encoded pulse-coupled oscillators*, International Journal of Wireless Information Networks, 16 (2009), pp. 51–58.

[10] A. DÍAZ-GUILERA, C. J. PÉREZ, AND A. ARENAS, *Mechanisms of synchronization and pattern formation in a lattice of pulse-coupled oscillators*, Physical Review E, 57 (1998), p. 3820.

[11] L. FAUST AND P. WESTON, *Degree-Day Prediction of Adult Emergence of Photinus carolinus (Coleoptera: Lampyridae)*, Environmental Entomology, 38 (2009), pp. 1505–1512.

[12] R. S. FISHER, W. V. E. BOAS, W. BLUME, C. ELGER, P. GENTON, P. LEE, AND J. ENGEL, *Epileptic seizures and epilepsy: Definitions proposed by the international league against epilepsy (ilae) and the international bureau for epilepsy (ibe)*, Epilepsia, 46 (2005), pp. 470–472.

[13] V. FLUNKERT, S. YANCHUK, T. DAHMS, AND E. SCHÖLL, *Synchronizing Distant Nodes: A Universal Classification of Networks*, Phys. Rev. Lett., 105 (2010), p. 254101.

[14] N. FUJIWARA, J. KURTHS, AND A. DÍAZ-GUILERA, *Synchronization in networks of mobile oscillators*, Phys. Rev. E, 83 (2011), p. 025101.

[15] D. GASCN AND M. YARZA, *Wireless sensor networks to control radiation levels*. `http://www.libelium.com/es/wireless_sensor_networks_to_control_radiation_levels_geiger_counters`, 2011.

[16] P. GOEL AND B. ERMENTROUT, *Synchrony, stability, and firing patterns in pulse-coupled oscillators*, Physica D, 163 (2002), pp. 191–216.

[17] X. GUARDIOLA, A. DIAZ-GUILERA, M. LLAS, AND C. PÉREZ, *Synchronization, diversity, and topology of networks of integrate and fire oscillators*, Physical Review E, 62 (2000), p. 5565.

[18] M. R. GUEVARA AND L. GLASS, *Phase locking, period doubling bifurcations and chaos in a mathematical model of a periodically driven oscillator: a theory for the entrainment of biological oscillators and the generation of cardiac dysrhythmias*, J. Math. Biol., 14 (1982), pp. 1–23.

[19] M. R. GUEVARA, A. SHRIER, AND L. GLASS, *Phase resetting of spontaneously beating embryonic ventricular heart cell aggregates*, Am. J. Physiol., 251 (1986), pp. H1298–1305.

[20] Y.-W. HONG AND A. SCAGLIONE, *Time synchronization and reach-back communications with pulse-coupled oscillators for uwb wireless ad hoc networks*, in Ultra Wideband Systems and Technologies, 2003 IEEE Conference on, IEEE, 2003, pp. 190–194.

[21] Y.-W. HONG AND A. SCAGLIONE, *A scalable synchronization protocol for large scale sensor networks and its applications*, IEEE J. Sel. Area Comm., 23 (2005), pp. 1085–1099.

[22] A. HU AND S. D. SERVETTO, *On the scalability of cooperative time synchronization in pulse-connected networks*, IEEE ACM T. Network., 52 (2006), pp. 2725–2748.

[23] G. IBEZ, E. MANZANEDO, J. A. CARRAL, A. GRACIA, AND J. M. ACRO, *A performance comparison of virtual backbone formation algorithms for wireless mesh networks*, (2009).

[24] J. KLINGLMAYR AND C. BETTSTETTER, *Synchronization of inhibitory pulse-coupled oscillators in delayed random and line networks*, in Applied Sciences in Biomedical and Communication Technologies (ISABEL), 2010 3rd International Symposium on, nov. 2010, pp. 1 –5.

[25] J. KLINGLMAYR, C. KIRST, C. BETTSTETTER, AND M. TIMME, *Guaranteeing global synchronization in networks with stochastic interactions*, New Journal of Physics, 14 (2012), p. 073031.

[26] ——, *Guaranteeing global synchronization in networks with stochastic interactions*, New Journal of Physics, 14 (2012), p. 073031.

[27] K. KONISHI AND H. KOKAME, *Synchronization of pulse-coupled oscillators with a refractory period and frequency distribution for a wireless sensor network*, Chaos, 18 (2008), p. 033132.

[28] Y. KURAMOTO, *International symposium on mathematical problems in theoretical physics, vol. 39 in lecture notes in physics*, (1975).

[29] A. D. M. ZEITLER AND C. GIELEN, *Asymmetry in pulse-coupled oscillators with delay*, Phys. Rev. E, 79 (2009).

[30] E. MALLADA, X. MENG, M. HACK, L. ZHANG, AND A. TANG, *Skewless network clock synchronization*, arXiv preprint arXiv:1208.5703, (2012).

[31] E. MALLADA AND A. TANG, *Synchronization of phase-coupled oscillators with arbitrary topology*, in American Control Conference (ACC), 2010, IEEE, 2010, pp. 1777–1782.

[32] ——, *Distributed clock synchronization: Joint frequency and phase consensus*, in Decision and Control and European Control Conference (CDC-ECC), 2011 50th IEEE Conference on, IEEE, 2011, pp. 6742–6747.

[33] R. E. MIROLLO AND S. H. STROGATZ, *Synchronization of pulse-coupled biological oscillators*, SIAM J. Appl. Math., 50 (1990), pp. 1645–62.

[34] M. MITCHELL, *An Introduction to Genetic Algorithms*, MIT Press, Cambridge, MA, USA, 1998.

[35] R. MOTWANI AND P. RAGHAVAN, *Randomized algorithms*, Cambridge university press, 1995.

[36] J. NISHIMURA AND E. FRIEDMAN, *Learning Phase Response Curves to Reach Synchrony*, In Preparation, (2011).

[37] J. NISHIMURA AND E. J. FRIEDMAN, *Robust convergence in pulse-coupled oscillators with delays*, Phys. Rev. Lett., 106 (2011), p. 194101.

[38] J. NISHIMURA AND E. J. FRIEDMAN, *Probabilistic convergence guarantees for type-ii pulse-coupled oscillators*, Physical Review E, 86 (2012), p. 025201.

[39] F. NUNEZ, Y. WANG, S. DESAI, G. CAKIADES, AND F. J. DOYLE, *Bio-inspired synchronization of wireless sensor networks for acoustic event detection systems*, in Precision Clock Synchronization for Measurement Control and Communication (ISPCS), 2012 International IEEE Symposium on, IEEE, 2012, pp. 1–6.

[40] M. PENROSE, *Random geometric graphs*, Oxford studies in probability, Oxford University Press, 2003.

[41] C. S. PESKIN, *Mathematical aspects of heart physiology*, Courant Institute of Mathematical Sciences, New York University New York, 1975.

[42] J. PODPORA, L. REZNIK, AND G. VON PLESS, *Intelligent real-time adaptation for power efficiency in sensor networks*, Sensors Journal, IEEE, 8 (2008), pp. 2066–2073.

[43] PROCEEDINGS OF THE 6TH INTERNATIONAL CONFERENCE ON INFORMATION PROCESSING IN SENSOR NETWORKS, *DESYNC: self-organizing desynchronization and TDMA on wireless sensor networks*, 2007.

[44] M. SCHMIDT AND H. LIPSON, *Distilling free-form natural laws from experimental data*, science, 324 (2009), pp. 81–85.

[45] M. D. SCHMIDT, R. R. VALLABHAJOSYULA, J. W. JENKINS, J. E. HOOD, A. S. SONI, J. P. WIKSWO, AND H. LIPSON, *Automated refinement and inference of analytical models for metabolic networks*, Physical biology, 8 (2011), p. 055011.

[46] R. M. SMEAL, G. B. ERMENTROUT, AND J. A. WHITE, *Phase-response curves and synchronized neural networks*, Philos. Trans. R. Soc. Lond. B, 365 (2010), pp. 2407–2422.

[47] H. M. SMITH, *Synchronous flashing of fireflies*, Science, 82 (1935), pp. 151–152.

[48] S. H. STROGATZ, *Sync: The emerging science of spontaneous order*, Hyperion, 2003.

[49] T. TATENO AND H. P. C. ROBINSON, *Phase resetting curves and oscillatory stability in interneurons of rat somatosensory cortex*, Biophys. J., 92 (2007), pp. 683–695.

[50] M. TIMME AND F. WOLF, *The simplest problem in the collective dynamics of neural networks: is synchrony stable?*, Nonlinearity, 21 (2008), p. 1579.

[51] M. TIMME, F. WOLF, AND T. GEISEL, *Coexistence of regular and irregular dynamics in complex networks of pulse-coupled oscillators*, Physical review letters, 89 (2002), p. 258701.

[52] X. WANG, R. K. DOKANIA, AND A. APSEL, *PCO-Based Synchronization for Cognitive Duty-Cycled Impulse Radio Sensor Networks*, IEEE Sensors Journal, 11 (2011), pp. 555–564.

[53] Y. WANG AND F. DOYLE, *Optimal phase response functions for fast pulse-coupled synchronization in wireless sensor networks*, (2012).

[54] Y. WANG, F. NUNEZ, AND F. J. DOYLE III, *Energy-efficient pulse-coupled synchronization strategy design for wireless sensor networks through reduced idle listening*, (2012).

[55] A. T. WINFREE, *The geometry of biological time.*, Springer-Verlag, 1980.

[56] W. WU AND T. CHEN, *Desynchronization of pulse coupled oscillatros with delayed excitatory coupling*, Nonlinearity, 20 (2007).